Partial Reactions of the Na,K-ATPase: Determination of Rate Constants

STEPHAN HEYSE, INGO WUDDEL, HANS-JÜRGEN APELL, and WERNER STÜRMER

From the Department of Biology, University of Konstanz, D-78434 Konstanz, Germany

ABSTRACT Experiments were designed to characterize several partial reactions of the Na,K-ATPase and to demonstrate that a model can be defined that reproduces most of the transport features of the pump with a single set of kinetic parameters. We used the fluorescence label 5-iodoacetamidofluorescein, which is thought to be sensitive to conformational changes, and the styryl dye RH 421, which can be applied to detect ion-binding and -release reactions. In addition transient electric currents were measured, which are associated mainly with the $E_1 \rightarrow E_2$ conformational transition. Numerical simulations were performed on the basis of a reaction model, that has been developed from the Post-Albers cycle. Analysis of the experimental data allows the determination of several rate constants of the pump cycle. Our conclusions may be summarized as follows: (*a*) binding of one Na^+ ion at the cytoplasmic face is electrogenic. This Na^+ ion is specifically bound to a neutral binding site with an affinity of 8 mM in the presence of 10 mM Mg^{2+}. In the absence of divalent cations, the intrinsic binding affinity was found to be 0.7 mM. (*b*) The analysis of fluorescence experiments with the cardiotonic steroid strophanthidin indicates that the 5-iodoacetamidofluorescein label monitors the conformational transition $(Na_3)E_1\text{-}P \rightarrow P\text{-}E_2(Na_2)$, which is accompanied by the release of one Na^+ ion. 5-IAF does not respond to the release of the subsequent two Na^+ ions, which can be monitored by the RH 421 dye. These experiments indicate further that the conformational transition $E_1P \rightarrow P\text{-}E_2$ is the rate limiting process of the Na^+ translocation. The corresponding rate constant was determined to be 22 s^{-1} at 20°C. From competition experiments with cardiotonic steroids, we estimated that the remaining 2 Na^+ ions are released subsequently with a rate constant of at least 5,000 s^{-1} from their negatively charged binding sites. (*c*) Comparing the fluorescence experiments with electric current transients, which were performed at various Na concentrations in the absence and presence of strophanthidin, we found that the transition $(Na_3)\cdot E_1\text{-}P \rightarrow P\text{-}E_2\cdot(Na_2)$ is the major charge translocating step in the reaction sequence $Na_3\cdot E_1 \rightarrow (Na_3)\cdot E_1\text{-}P \rightarrow P\text{-}E_2\cdot(Na_2) \rightarrow P\text{-}E_2$. The subsequent release of 2 Na^+ ions contributed less than 25% to the total electric current transient. (*d*) The well known antagonism between cardiotonic steroids and K^+

W. Stürmer's present address is Research Center for Pharmacology, Bayer AG, D-42096 Wuppertal, Germany.

Address correspondence to H.-J. Apell, Department of Biology, University of Konstanz, Postfach 5560 M635, D-78434 Konstanz, Germany.

J. GEN. PHYSIOL. © The Rockefeller University Press · 0022-1295/94/08/0197/44 $2.00
Volume 104 August 1994 197–240

binding can be explained by a kinetic model. A quantitative description has been obtained under the assumption that these inhibitors bind only to the states P-$E_2(Na_2)$ and P-$E_2(K_2)$. (*e*) Most of our experiments can be described by a modified Post-Albers scheme. A set of the kinetic parameters in this scheme has been determined by the experiments presented or by data from literature. Numerical simulations using this set are consistent with the presented data.

INTRODUCTION

The operation of the Na,K-pump involves a sequence of conformational transitions and ion binding and release reactions (Glynn, 1985; Jørgensen and Andersen, 1988). Biochemical characterization and proteolysis experiments indicate that the enzyme can assume two principal conformations designated as E_1 and E_2. In the E_1 conformation, the enzyme presents ion-binding sites to the cytoplasm and is stabilized by Na^+ ions. In E_2 the ion-binding sites face the extracellular side and the

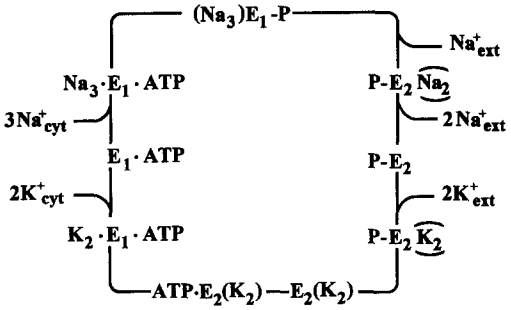

FIGURE 1. Post-Albers scheme of the pump cycle of the Na,K-ATPase, adapted from Läuger (1991). E_1 and E_2 are conformations of the enzyme with binding sites facing the cytoplasm and the extracellular medium, respectively. In the occluded states (Na_3) E_1-P, $E_2(K_2)$ and ATP·($E_2(K_2)$ the bound ions are unable to exchange with the aqueous phase. P-$E_2(K_2)$ and P-$E_2(Na_2)$ indicate states, which may occlude ions upon binding of cardiotonic steroids. Dashes indicate covalent bonds and dots indicate noncovalent bonds. When the enzyme is phosphorylated by ATP in state E_1, three Na^+ ions become occluded (Na_3·E_1·ATP → (Na_3)·E_1-P). The spontaneous transition to conformation E_2 leads to the release of the Na^+ ions to the extracellular side. The subsequent binding of potassium initiates enzyme dephosphorylation and occlusion of K^+ ions. Low-affinity binding of ATP shifts the conformation to state E_1 from which K^+ is released to the cytoplasm.

enzyme is stabilized by K^+ ions. The physiological function of the Na,K-pump can be described by the Post-Albers reaction cycle (Fig. 1).

The kinetics of several partial reactions have been studied by various techniques such as time-resolved phosphorylation and dephosphorylation studies (Mårdh and Zetterquist, 1974; Froehlich, Albers, Koval, Goebel, and Berman, 1976; Mårdh and Post, 1977; Hobbs, Albers, and Froehlich, 1988), time-resolved flux measurements on ion transport and (de)occlusion (Forbush, 1984; 1987*a*,*b*), studies on transient currents (Fendler, Grell, Haubs, and Bamberg, 1985; Nakao and Gadsby, 1986; Borlinghaus, Apell, and Läuger, 1987) or time-resolved fluorescence measurements (Karlish and Yates, 1978; Kapakos and Steinberg, 1982; Taniguchi, Suzuki, and Iida, 1983; Skou and Esmann, 1983; Rephaeli, Richards, and Karlish, 1986; Stürmer, Apell, Wuddel, and Läuger, 1989; Stürmer, Bühler, Apell, and Läuger, 1991*b*). Despite the large number of kinetic experiments, basic questions concerning the kinetics of partial reactions still remain open. However, there are at least two reasons

to determine the rate constants of partial reactions of the reaction cycle and their temperature dependence. (*a*) Experiments have been performed with enzyme prepared from various species, different tissues and at different temperatures. Recent experiments indicated that large divergence may occur between the rate constants of enzyme prepared from different species and of different enzyme isoforms (Forbush and Klodos, 1991; Sweadner, 1991). Because comprehensive information is scarce, both about species differences in rate constants and about their temperature dependence, a consistent set of parameters would permit a crucial analysis of proposed pump schemes.

(*b*) The knowledge of the forward and backward rate constants of all partial reactions allows the determination of basic free-energy levels. The determination of the temperature dependence of these rate constants allows the calculation of enthalpy and entropy terms of single reaction steps.

Such an analysis has been performed in part for the Na,K-pump (Läuger and Apell, 1986; Stürmer et al., 1989; Stein, 1990; Läuger, 1991). The analysis in these studies was based on the Post-Albers cycle. Since there was not enough detailed experimental information available, it had to be assumed: (*a*) the enzyme can bind up to three Na^+ ions or up to two K^+ ions. Mixed species such as $Na_{1,2}{\cdot}K{\cdot}E_i$ are excluded, (*b*) the three Na^+ sites were considered to be equivalent in their binding properties (the same assumption was made for the two K^+ sites), and (*c*) the rate constants for binding and release of Na^+ and K^+ ions were assumed to be large compared to other reaction steps so that the six different forms, Na_3E_1, Na_2E_1, . . ., K_2E_1, are always in equilibrium with each other.

There is now considerable experimental evidence to replace the second assumption. One line of evidence comes from electrophysiological experiments on whole cells, which suggest that Na^+ release (Gadsby, Rakowski, and De Weer, 1993) and K^+ binding (Lafaire and Schwarz, 1986; Rakowski, Vasilets, La Tona, and Schwarz, 1991) at the extracellular side is electrogenic and becomes rate limiting under conditions of low K^+ concentrations ($[K^+] < 0.1$ M) and of positive membrane potential.

These experiments are supplemented by fluorescence experiments with Na,K-ATPase membrane fragments. In these studies, styryl dyes such as RH 160 or RH 421 have been used to detect local changes of electric field-strength in open membrane fragments (Klodos and Forbush, 1988; Bühler, Stürmer, Apell, and Läuger, 1991; Stürmer et al., 1991*a,b;* Stürmer and Apell, 1992). These experiments suggest that cytoplasmic binding of an Na^+ ion, extracellular Na^+ release, and extracellular K^+ binding are electrogenic and, under appropriate conditions, rate limiting.

We will propose a more detailed reaction model, which takes these results into account. In the following optical and electric experiments are described, which were designed to characterize several of the partial reactions of the pump cycle. An ATP-concentration jump technique has been applied, which allowed us to study the time dependence of partial reactions of the Na,K-pump. To distinguish different states of the Na,K-pump, we used two methods based on the properties of two different fluorescence labels. (*a*) 5-Iodoacetamidofluorescein (5-IAF): this dye binds covalently to cys 457 on the cytoplasmic face of the protein (Tyson, Steinberg, Wallick, and Kirley, 1989). The characteristic fluorescence changes of this dye, which may be observed upon changes of the composition of the medium, are thought to

reflect conformational changes of the protein (Glynn, Hara, Richards, and Steinberg, 1987; Steinberg and Karlish, 1989; Stürmer et al., 1989). With our preparation of enzyme from rabbit kidney it is possible to discriminate between three different groups of enzyme states: (1) all E_1 states, including $(Na_3)E_1$-P, (2) all P-E_2 states and (3) $E_2(K_2)$ and ATP·$E_2(K_2)$ (Stürmer et al., 1989).

(*b*) RH 421: this amphiphilic electrochromic styryl dye is thought to insert in lipid domains of Na,K-ATPase membrane fragments. It does not respond to conformational transitions but detects changes of electric field strength inside the membrane dielectric. Such changes in electric field strength are caused by binding or release of ions and/or by movement of charge inside the membrane and allow this way a discrimination between differently charged states of the enzyme (Bühler et al., 1991). The mechanism is not completely elucidated so far (see below).

MATERIALS AND METHODS

Materials

Sodium dodecylsulfate (SDS) was obtained from Pierce Chemical Co. (Rockford, IL), sodium cholate from Merck (Darmstadt, Germany) and diphytanoyllecithin from Avanti Polar Lipids, Inc. (Birmingham, AL). Phosphoenolpyruvate, pyruvate kinase, lactate dehydrogenase, luciferin, luciferase, NADH and ATP (disodium salt, Sonderqualität) were from Boehringer GmbH (Mannheim, Germany). α-chymotrypsin (type IV), apyrase VI and strophanthidin were purchased from Sigma (München, Germany). 5-Iodoacetamidofluorescein (5-IAF), RH 421 and P^3-1-(2-nitro) phenylethyladenosine-5′-triphosphate ("caged" ATP) were obtained from Molecular Probes Inc. (Eugene, OR). The purity of these products was checked by thin-layer chromatography. Ethylenediamine tetraacetic acid (EDTA) and NaCl were from Merck. In experiments with a nominal absence of K^+, NaCl was used in Suprapur quality. All other reagents were of analytical grade. Sephadex G25 was obtained from Serva (Heidelberg, Germany).

Enzyme preparation and fluorescence labeling. Na,K-ATPase was prepared from the outer medulla of rabbit kidneys using procedure C of Jørgensen (1974). This method yields purified enzyme in the form of membrane fragments containing ~0.8 mg phospholipid and 0.2 mg cholesterol per mg protein (Bühler et al., 1991). The specific ATPase activity was determined by the pyruvate kinase/lactate dehydrogenase assay (Schwartz, Nagano, Nakao, Lindenmayer, and Allen, 1971). Pyruvate kinase and lactate dehydrogenase were added in a 100-fold excess over ATPase activity. The protein concentration was determined by the Lowry method (Lowry, Rosebrough, Farr, and Randall, 1951), using bovine serum albumin as a standard. For most preparations the specific activity was in the range between 1,500 and 2,500 μmol P_i per h and mg protein at 37°C, corresponding to a turnover rate of 60–85 s^{-1} (based on a molar mass of 140,000 g/mol). The suspension of Na,K-ATPase-rich membrane fragments (~3 mg protein/ml) in buffer (25 mM imidazole sulfate, pH 7.5, 1 mM EDTA, 10 mg/ml sucrose) was frozen in samples of 100 μl; in this form the preparation could be stored for several months at −70°C without significant loss of activity.

Labeling of the enzyme with 5-IAF was performed by incubating 200–300 μg of the enzyme for 48 h at 4°C with a solution containing 100 μM 5-IAF, 10 mM K_2SO_4 and 50 mM imidazole sulfate, pH 7.5 (Kapakos and Steinberg, 1982). The labeled enzyme was separated from unbound dye by passing the reaction mixture through a Sephadex G-25 column of 5 cm length. The specific activity was not significantly changed by the labeling procedure.

In the experiments with RH 421, the dye was added from an ethanolic stock solution to the aqueous suspension of membrane fragments to obtain a final concentration of 200 nM. In

contrast to 5-IAF the styryl dye RH 421 is not linked to the protein but dissolved in the membrane dielectric and aligned with the negatively charged sulfonate end towards the aqueous phase. Due to the high partition coefficient of the styryl dye, ~90% was bound to the membrane fragments (Bühler et al., 1991). Although there is general agreement that RH styryl dyes respond to changes of the electric field in the membrane, the mechanism is not explained completely so far (Grinwald, Hildesheimer, Farber, and Anglister, 1982; Bühler et al., 1991; Clarke, Schrimpf, and Schöneich, 1992). While Bühler et al. (1991) attributed the main effect to an electrochromic mechanism, Clarke et al. (1992) presented evidence for additional voltage-sensitive aggregation of dye molecules. According to Clarke et al. (1992) the differences and their explanations may be due to higher dye concentrations they used compared to Bühler et al. (1991). Conformational rearrangements of the enzyme which are not associated with charge movements in the protein do not contribute to fluorescence intensity changes (Bühler et al., 1991; Stürmer et al., 1991*b*).

Steady state fluorescence and absorption measurements. Most steady state fluorescence measurements were carried out with a fluorescence spectrophotometer (model 650-40, Perkin-Elmer Cetus Corp., Norwalk, CT). The thermostated cell holder was equipped with a magnetic stirrer. For experiments with RH 421, the excitation wavelength was set to 580 nm (slit width 15 nm) and the emission wavelength to 660 nm (slit width 15 nm). For some experiments with the dye RH 421, we used a home-built fluorescence spectrometer. The excitation and emission wavelengths were selected with interference filters (λ_{ex} = 580, λ_{em} = 660 nm, bandwidth 9 nm). 5-IAF fluorescence was excited at 480 nm (slit width 10 nm), emission was monitored at 520 nm (slit width 10 nm). Binding of anthroylouabain was studied at λ_{ex} = 365 nm (slit width 10 nm) and λ_{em} = 510 nm (slit width 10 nm). Absorption measurements were performed with a Perkin-Elmer Lambda 5 spectrophotometer. If not otherwise indicated, the experiments were carried out at 20°C.

Measurement of transient fluorescence signals after photochemical release of ATP. Transient fluorescence signals produced by photochemical release of ATP were measured as described previously (Stürmer et al., 1989). The optical cell was filled with 200–300 μl of a suspension of membrane fragments (usually 5–30 μg protein/ml) in a medium containing 30 mM imidazole, pH 7.2, 1 mM EDTA, fluorescence dye and various amounts of NaCl and KCl. The fluorescence was excited by light from a 250 W tungsten-halogen lamp. Fluorescence light emitted from the sample cell was collected by an ellipsoidal mirror and focused onto the cathode of the photo multiplier. Excitation and emission wavelength were selected by interference filters (band-width is ~13 nm).

The current signal of the photo multiplier was converted to voltage and amplified in three stages. The input stages of the amplifiers were protected by diodes against overload. This was necessary since the 308 nm laser flash excited fluorescence and phosphorescence in some of the optical elements (lenses and cuvette), which decayed with a time constant of ~1 ms. For compensation of the stationary fluorescence signal before the flash, a differential amplifier was used. The output signal was amplified 10-fold. The signal was digitized by a 16-bit analogue-to-digital converter (DSP 32C Loughborough Sound Images Ltd., Loughborough, Leics LE11 0QE, UK) and stored on the hard disk of a personal computer.

ATP was released from "caged" ATP (cg-ATP) in the cuvette by a light flash (wavelength 308 nm, total energy 150 mJ, duration 10 ns) generated by an EMG 100 excimer laser (Lambda Physics, Göttingen). At pH 7.0 ATP is set free from cg-ATP with a time constant of 4.6 ms (McCray, Herbette, Kihara, and Trentham, 1980). The concentration of released ATP was determined by the luciferin/luciferase test which was calibrated using solutions of known ATP concentration (DeLuca and McElroy, 1978). If not stated otherwise, the initial concentration of cg-ATP was 100 μM from which ~ 15–25 μM ATP were released by a single flash. To remove

traces of free ATP from the sample of cg-ATP, a small amount of apyrase (10^{-3} U/ml) and 2 mM Mg^{2+} were added to the stock solution of cg-ATP.

Recording of electric signals. The method for measurement of transient electric currents, which result from charge translocation within the membrane dielectric, has been described previously (Borlinghaus et al., 1987; Stürmer et al., 1989). Optically black films were formed from a solution of 10 mg/ml diphytanoylphosphatidylcholine in *n*-decane (Läuger, Lesslauer, Marti, and Richter, 1967). The membrane cell was made of Teflon and consisted of two compartments separated by a thin Teflon septum with a circular hole of 1.0-mm diam. When a suspension of membrane fragments was added to one of the compartments, fragments became bound to the bilayer and covered up to 50% of the bilayer surface (Fringeli, Apell, Fringeli, and Läuger, 1989). The solutions on either side of the lipid membrane were connected to the external measuring circuit via agar bridges and silver/silver-chloride electrodes. For current measurements under short-circuit conditions, the signal was amplified with a current amplifier (Keithley model 427). For measuring voltage signals, a model 3528 Burr-Brown amplifier with an input impedance of 10^{12} Ω was used. The signals were recorded with a digital oscilloscope (Nicolet model 4094 A) and stored on diskettes. If not indicated otherwise, the aqueous solutions contained 30 mM imidazole, pH 7.2, 10 mM $MgCl_2$, 1 mM EDTA and the indicated concentration of NaCl. Cg-ATP (usually 250 μM) and membrane fragments (about 50 μg protein/ml) were added together to one of the compartments.

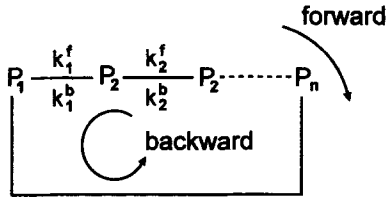

FIGURE 2. Transitions between states P_1, P_2, ... P_{n-1}, P_n of a pump molecule. k_1^f, k_2^f, ... and k_1^b, k_2^b, ... are rate constants for transitions in forward and backward direction, respectively.

Light flashes of 40 μs duration and a total energy of 5 J were generated with a Xenon flash-tube (model 5M-3) from EG&G Electro-Optics (Salem, MA). The emitted light passed through a bandpass filter with a transparency of >50% between 260 and 380 nm (model UG11, Schott, Mainz, Germany). From the recorded current transients, $I(t)$, the pump current, $I_p(t)$, has been determined by a previously published method (Borlinghaus et al., 1987). The amount of charge, $Q(t)$ was calculated by integration of $I_p(t)$ between $t = 0$ and the required time t.

Numerical simulation of the fluorescence changes and current transients. The method used to evaluate the time course of the relative fluorescence change ($\Delta F/F_0$) can be described on the basis of a general scheme (Fig. 2), in which it is assumed that operation of the pump involves a sequence of transitions between states P_i ($i = 1, 2, \ldots n$). The rate constants k_i^f and k_i^b in forward and backward direction are in general pseudo-monomolecular rate constants and may contain substrate concentrations. x_i (t) is defined as the fraction of enzyme in state P_i at time t. The time derivative of x_i is given by:

$$\frac{dx_i}{dt} = -(k_{i-1}^b + k_i^f)\cdot x_i + k_{i-1}^f \cdot x_{i-1} + k_{i+1}^b \cdot x_{i+1} \qquad (i = 1, 2, \ldots, n). \tag{1}$$

The functions x_i (t) can be obtained by numerical integration of the n coupled Eq. 1.

Defining φ_i as the fluorescence induced by one enzyme molecule in state P_i and N as the

number of fluorescence molecules, the measured fluorescence F may be noted as:

$$F = N \cdot \sum_i \varphi_i \cdot x_i. \tag{2}$$

With $F_o = F(t = 0)$ and $x_{io} = x_i(t = 0)$, the relative fluorescence change $\Delta F/F_0$ can be defined as:

$$\frac{\Delta F(t)}{F_o} = \frac{\sum_i \varphi_i \cdot (x_i(t) - x_{io})}{\sum_i \varphi_i \, x_{io}}. \tag{3}$$

In order to describe the time dependence of the transient pump current, $I_p(t)$, we introduce the net rate $\Phi(t)$ of transition between states $P_i \rightarrow P_{i+1}$ (Fig. 2):

$$\Phi_i(t) = k_i^f \cdot x_i - k_{i+1}^b \cdot x_{i+1}. \tag{4}$$

The charge movement $Q(t)$ inside the protein dielectric may be written as:

$$Q(t) = \int_0^t I_p(t)\, dt = e_o \cdot N \cdot \sum_i \left(\alpha_i \cdot \int_0^t \Phi_i(t)\, dt \right) = \sum_i q_i(t). \tag{5}$$

$I_p(t)$ is the pump current, e_o the elementary charge, and N is the number of pump molecules which contribute to the signal. α_i are dielectric coefficients which account for the dielectric length of the charge movement (Läuger and Apell, 1986). The $q_i(t)$ are the contributions of the individual reaction steps to the entire charge transient.

The pump cycle: basic assumptions. The model applied in all numerical descriptions of the pump cycle is illustrated in Fig. 3. It is based on the Post-Albers scheme (Fig. 1) and has been expanded in order to account for (*a*) noncanonical flux modes; (*b*) recent findings, which indicate that Na^+ release and K^+ binding at the extracellular face are electrogenic and possibly involve migration of 2 Na^+ or 2 K^+ ions along a narrow access channel (Stürmer et al., 1991*b*; Rakowski et al., 1991; "ion well," Läuger, 1991); and (*c*) the finding that on the cytoplasmic side binding of a Na^+ is electrogenic in contrast to K^+ binding. We still assume that binding or release of 2 Na^+ and 2 K^+ ions is fast on the cytoplasmic face. This is formalized by the assumption that these states are in equilibrium with each other at all times (Läuger and Apell, 1988):

$$\frac{x[Na_i \cdot E_1]}{x[Na_{i-1} \cdot E_1]} = \frac{x[Na_i \cdot E_1 \cdot ATP]}{x[Na_{i-1} \cdot E_1 \cdot ATP]} = \frac{c'_{Na}}{K_{Na,i}} \equiv n'_i \qquad (i = 1, 2) \tag{6}$$

$$\frac{x[K_j \cdot E_1]}{x[K_{j-1} \cdot E_1]} = \frac{x[K_j \cdot E_1 \cdot ATP]}{x[K_{j-1} \cdot E_1 \cdot ATP]} = \frac{c'_K}{K_{K,j}} \equiv k'_j \qquad (j = 1, 2). \tag{7}$$

$x[P_i]$ denotes the fraction of molecules in state P_i, c'_{Na} is the cytoplasmic concentration of Na^+, c'_K the cytoplasmic concentration of K^+. $K_{Na,i}$ and $K_{K,j}$ are equilibrium dissociation constants.

This assumption is supported by experiments in which evidence is presented that the negatively charged (unselective) binding sites for these ions are located presumably at the protein-water interface (Grell et al., 1991; Stürmer et al., 1991*a*,*b*). The term "binding sites are located at the protein-water interface," which is used in this study, does not necessarily imply a location at the topological protein-water interface. They can be located also in a water-filled vestibule, as long as the electric field strength resulting from a transmembrane voltage is low within the vestibule.

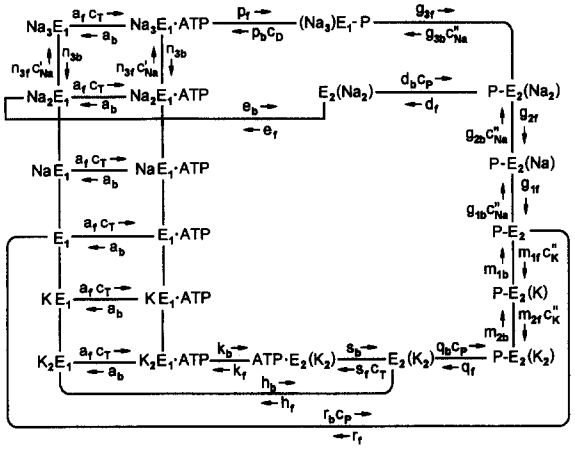

FIGURE 3. Expanded form of the Post-Albers cycle (Fig. 1) for the evaluation of the time dependence of $\Delta F/F_o$ and $Q(t)$. a_f, p_f, ... a_b, p_b, ... are rate constants in forward and backward direction, respectively. c_T, c_D, and c_P are concentrations of ATP, ADP and P_i. c'_{Na}, c'_K, c''_{Na}, c''_K are the concentrations of Na^+ and K^+ at the cytoplasmic and extracellular side, respectively.

RESULTS

In this section a series of experiments are described that allowed us to determine independently sets of rate constants by appropriate experimental conditions and techniques. The sequence of paragraphs follows the Post-Albers cycle of Fig. 3.

Cytoplasmic Sodium Binding in the Absence of K^+ and ATP

Sodium binding to the unphosphorylated enzyme was investigated at high and low ionic strength with the 5-IAF and RH 421 method. Data from the literature indicate that in the absence of alkali ions the protein is forced by high ionic strength into an E_1 conformation, in low ionic strength the protein is expected to be stabilized mainly in an E_2 conformation (Grell et al., 1991; David and Karlish, 1990).

In high ionic strength (0.4 M choline chloride), addition of Na^+ does not change the fluorescence of the 5-IAF-labeled enzyme. At low ionic strength, addition of Na^+ to the IAF-labeled enzyme leads to a fluorescence increase of ~8% (Fig. 4). This change of 5-IAF fluorescence is not sodium specific and can be obtained also with cations like choline, guanidinium or imidazole. The time constant of the fluorescence

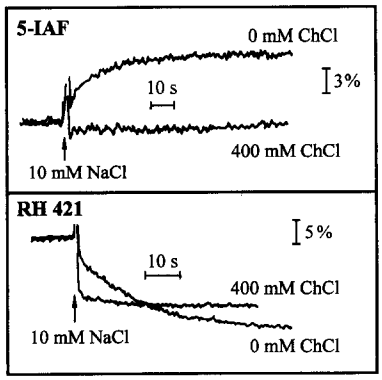

FIGURE 4. High affinity Na^+ binding at low and high ionic strength. RH 421 or 5-IAF-labeled membrane fragments were incubated in a solution containing 5 mM histidine, 0.1 mM EDTA, 10 mM $MgCl_2$ and 0 or 400 mM choline chloride. 10 mM NaCl was added from a 1 M stock solution.

increase was determined to be $\sim 0.2\ s^{-1}$ (Fig. 4 *top*). This value is similar to the values given in the literature for the conformational change from E_2 to E_1 and the rates of spontaneous deocclusion of Rb^+ (Karlish, 1980; Glynn and Richards, 1982; Forbush, 1987*b*). These data support the notion that in the absence of ATP and P_i, the enzyme is mainly in an E_2 conformation in buffer of low ionic strength, whereas high ionic strength stabilizes an E_1 conformation.

Addition of NaCl to RH 421-labeled fragments led to a fluorescence decrease in media of high and low ionic strength (Fig. 4, *bottom*). In contrast to experiments with the 5-IAF-labeled enzyme a fluorescence decrease with RH 421 could not be obtained with other cations (Li^+, K^+, Rb^+, Cs^+, NH_4^+, choline$^+$, guanidinium derivatives). The amplitude of the Na^+-induced fluorescence decrease was less affected by ionic strength (additional 2–5%) whereas the time course of these signals strongly depended on ionic strength. At low ionic strength, the time course was comparable to the time course measured with the 5-IAF-labeled enzyme and seems to be controlled

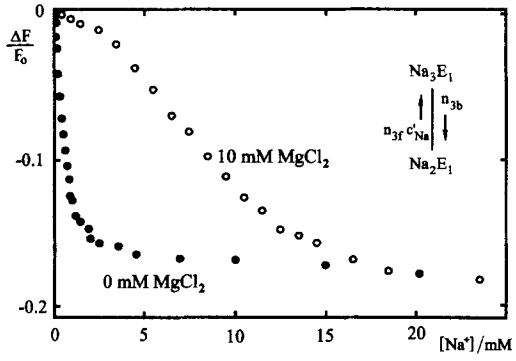

FIGURE 5. Relative fluorescence change $\Delta F/F_o$ of RH 421-labeled membrane fragments after addition of NaCl in the absence and presence of 10 mM $MgCl_2$ as a function of Na^+ concentration. A suspension of membrane fragments (30 μg/ml) was added to a solution containing 200 nM RH 421, 300 mM choline chloride, 25 mM histidine, 0.5 mM EDTA, pH 7.2 and the indicated concentration of $MgCl_2$. NaCl was added from a stock solution containing 300 mM NaCl, 25 mM histidine and 0.5 mM EDTA. The data are corrected for dilution effects. F_o is the fluorescence intensity before the addition of NaCl.

by the transition $E_2 \rightarrow E_1$. In high ionic strength media (>400 mM), addition of Na^+ led to a fast fluorescence decrease which could not be resolved even at low temperatures.

In the experiments shown in Fig. 5, RH 421-labeled fragments were titrated with NaCl in a buffer containing 25 mM histidine, 0.5 mM EDTA, 300 mM choline chloride, and 0 or 10 mM Mg^{2+}. The intrinsic binding affinity for sodium depended on the presence of divalent cations. In the presence of 10 mM Mg^{2+} the intrinsic equilibrium dissociation constant is 8 mM, without Mg^{2+} it is 0.7 mM. These values were not affected appreciably by low ionic strength. Experiments with other divalent cations like Ba^{2+} and Ca^{2+} gave similar results (data not shown).

From literature values (Froehlich and Fendler, 1991) and our own unpublished stopped flow experiments we estimated the rate constant n_{3f} to be $1 \cdot 10^5\ s^{-1}\ M^{-1}$ (as a lower limit). With the experimentally determined dissociation constant of 8 mM the backward rate constant n_{3b} can be calculated to be $800\ s^{-1}$.

ATP-concentration Dependence of the $E_1 \rightarrow E_2$ Conformational Transition

With regard to the conformational transition $E_1 \rightarrow E_2$, the apparent affinity for ATP may be determined with both 5-IAF and RH 421-labeled membrane fragments. In these experiments, labeled membrane fragments were incubated in the presence of 100 mM NaCl, 25 mM histidine, 0.5 mM EDTA, 10 mM $MgCl_2$ and various concentrations of cg-ATP. ATP was released from cg-ATP at time $t = 0$. This reaction triggered enzyme phosphorylation and the conformational transition to $P-E_2$ states. In Fig. 6 the ATP-concentration dependence of the amplitudes and the time course

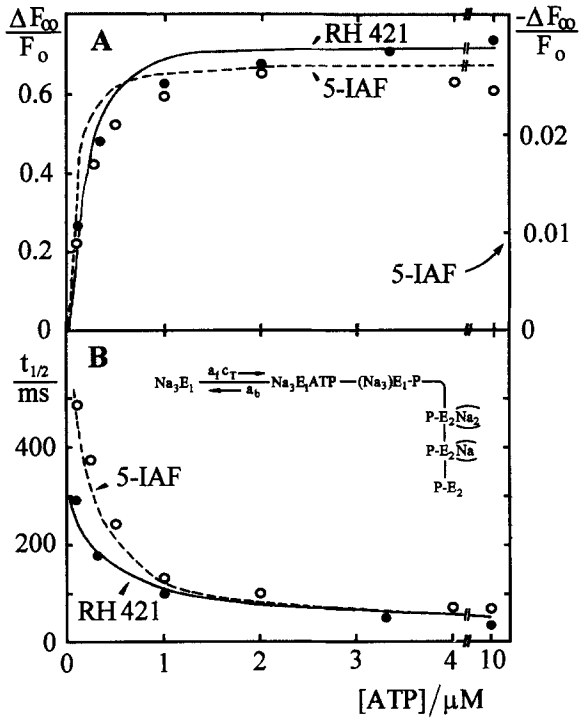

FIGURE 6. (*A*) Amplitudes $a_F \equiv \Delta F/F_o$ and (*B*) half times $t_{1/2}$ of ATP-induced fluorescence changes under K^+ free conditions as a function of ATP concentration. $t_{1/2}$ is the time at which $\Delta F(t)/F_o$ reaches its half-maximal value. F_o is the fluorescence intensity before the light flash. Experimental data are represented by circles. ATP was released from cg-ATP by a 308 nm light flash with a yield of ~20%. (*Open circles* ○) Suspension of 5-IAF-labeled membrane fragments (6 μg/ml) in 100 mM NaCl, 25 mM histidine, 0.5 mM EDTA, 10 mM $MgCl_2$ and the indicated concentration of ATP. (*Filled circles* ●) 200 nM RH 421 was added to a solution containing 30 μg/ml membrane fragments in 100 mM NaCl, 25 mM histidine, 0.5 mM EDTA, 10 mM $MgCl_2$ and the indicated concentration of ATP. The temperature was 20°C. The lines have been obtained by numerical simulations of the reaction cycle of Fig. 3 using the values given in Table V.

of the 5-IAF and RH 421 fluorescence signals are shown. In the absence of Mg^{2+} no fluorescence changes have been observed. At high concentrations ATP binding will be fast compared to the conformational transition $E_1 \rightarrow E_2$, and the half time for transition, $t_{1/2}$, reflects mainly either the rate of the conformational transition (5-IAF) or the rate of charge movement within the dielectric (RH 421). ATP binding became rate limiting in low ATP concentrations and determined the rate constant of the fluorescence change. At low ATP concentrations the fluorescence amplitude also decreased. This can be explained by the assumption that the rate of enzyme phosphorylation is reduced at low ATP concentrations whereas the rate of dephos-

phorylation presumably is unaffected by a change in ATP concentration. As a consequence only part of the enzyme is phosphorylated in the presence of low concentrations of ATP. The data in Fig. 6 show that the fluorescence change was half maximal at 50–100 nM and the conformational transition rate was half maximal at ~1 μM ATP. To make sure that ATP consumption does not reduce the actual concentration in a way that kinetic parameters determined in the presence of low ATP concentrations are changed, the experiments have been repeated with reduced enzyme concentration. A larger excess of ATP compared to the amount of protein led to the same results.

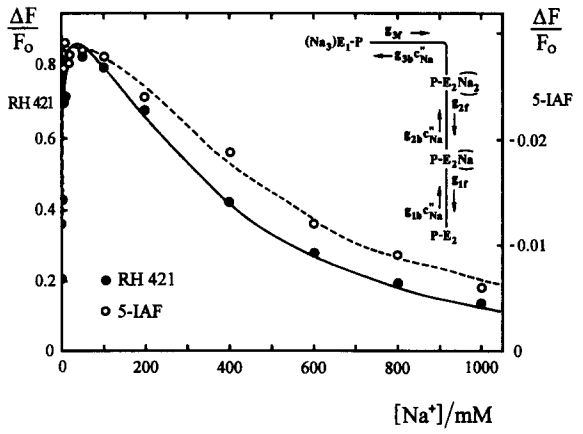

FIGURE 7. Amplitudes $\Delta F/F_o$ of ATP-induced fluorescence changes under K^+ free conditions as a function of Na^+ concentration. (*Open circles* ○) Suspension of 5-IAF-labeled membrane fragments (6 μg/ml) in 25 mM histidine, 0.5 mM EDTA, 10 mM $MgCl_2$, 100 μM cg-ATP and the indicated concentration of NaCl. (*Filled circles* ●): 200 nM RH 421 were added to a solution containing 30 μg/ml membrane fragments in 25 mM histidine, 0.5 mM EDTA, 10 mM $MgCl_2$, 100 μM cg-ATP and the indicated Na^+ concentration. 20 μM ATP was released from cg-ATP. The temperature was 20°C. The lines have been obtained by numerical simulations of the reaction cycle of Fig. 3.

Sodium-Concentration Dependence of the ATP-induced Fluorescence Change

The amplitude of the fluorescence signal, which was observed upon phosphorylation by saturating concentration of ATP (~20 μM), is plotted in Fig. 7 as a function of Na^+ concentration for the 5-IAF and RH 421 fluorescence signal. The relative fluorescence change $\Delta F/F_o$ reached a maximum at ~40 mM Na^+ and declined at higher Na^+ concentrations (Stürmer et al., 1991*b*).

The biphasic shape of the Na^+ concentration dependence of the fluorescence signal in Fig. 7 is presumably caused by two processes: the increasing fluorescence, $\Delta F/F_0$, up to 40 mM Na^+ can be attributed to the cytoplasmic activation of enzyme phosphorylation by Na^+, which is known to require only millimolar Na^+ concentrations. The region where the fluorescence change declines with increasing Na^+ (>40 mM Na^+) is thought to result from the successive equilibrium occupation of the binding sites in states P-E_2·(Na), P-E_2·(Na_2), and (Na_3)·E_1-P. The binding affinity of Na^+ on the extracellular side is known to be much lower than on the cytoplasmic side (Kaplan and Hollis, 1980; Kaplan, 1982).

The rate constant which controls enzyme phosphorylation, p_f, cannot be measured directly, because the step $Na_3E_1ATP \rightarrow (Na_3)E_1$-$P$ does not produce a change of the

RH 421 fluorescence. However, in the presence of ATP and of low Na^+ concentrations the state Na_3E_1ATP is populated only poorly and the transition to $(Na_3)E_1$-P becomes the rate limiting step in the whole reaction sequence after the experiment is started by an ATP concentration jump (~20 μM from 100 μM cg-ATP). The subsequent reaction steps, which are monitored by RH 421, are fast under these conditions ([Na^+] < 5 mM). A variation of the Na^+ concentration modulates the reaction flux through transition $Na_3E_1ATP \rightarrow (Na_3)E_1$-$P$ and, therefore, the analysis of the time course of these experiments can be used to get information on the rate constant p_f. In Fig. 8 the relative fluorescence amplitudes and the time course of the ATP-induced 5-IAF and RH 421 fluorescence signals are plotted as a function of Na^+

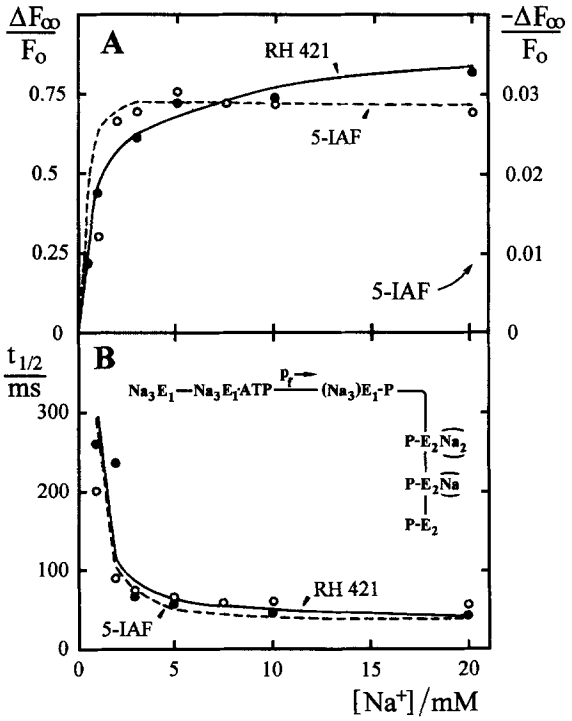

FIGURE 8. (*A*) Amplitude $\Delta F_\infty/F_0$ and (*B*) half time $t_{1/2}$ of ATP-induced fluorescence changes under K^+-free conditions as a function of Na^+ concentration between 1 mM and 20 mM. The experimental conditions were the same as in Fig. 7.

concentration (0–20 mM Na). With respect to the fluorescence amplitudes a half saturating concentration of 1–2 mM Na^+ was obtained (Fig. 8 *A*). A plot of reciprocal values of $t_{1/2}$ of the fluorescence time courses against [Na^+] yielded a K_M of 4 mM (Fig. 8 *B*).

Fluorescence Signals Associated with Na^+ Release to the Extracellular Side

The decrease of the stationary fluorescence signals at high Na^+ concentrations can be analyzed in terms of bound Na^+ (RH 421) and of the ratio of the population of $(Na_3)E_1$-P and phosphorylated states of E_2 (5-IAF). Changes of the fluorescence amplitudes were not significantly affected, when the ionic strength had been kept

constant at 1 M by addition of choline chloride. However, apparent affinities of the individual Na^+ release steps cannot be determined in an unambiguous way from these experiments. Therefore, different approaches were used to determine the kinetic and electrogenic properties of the Na^+ release steps.

Time dependence of extracellular sodium release. The time course of the 5-IAF and RH 421 fluorescence signals, which are associated with the conformational change $E_1 \rightarrow E_2$ and with the release of Na^+ ions to the extracellular side, can be measured easily with the ATP concentration jump technique. In Fig. 9 such experiments are shown using the 5-IAF and RH 421 method. Both experiments were carried out in the presence of 100 mM NaCl, 25 mM histidine, 0.5 mM EDTA, 10 mM $MgCl_2$, 100 μM cg-ATP and in the absence of K^+. The rise of the RH 421 fluorescence signal was significantly faster ($t_{1/2}$ = 40 ms) than of the 5-IAF signal ($t_{1/2}$ = 55 ms). Similar results were obtained using stopped-flow technique (Bühler, 1992). The same

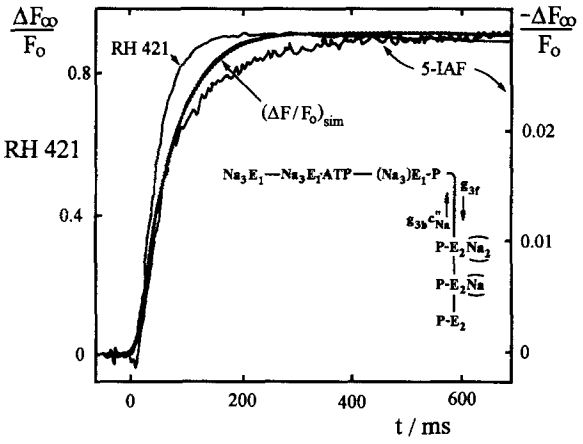

FIGURE 9. Time course of the relative fluorescence change $\Delta F(t)/F_0$ of RH 421 or 5-IAF-labeled membrane fragments after phosphorylation by ATP in the presence of 100 mM NaCl, 25 mM histidine, 0.5 mM EDTA, 10 mM $MgCl_2$ and 100 μM cg-ATP. About 20 μM ATP were released photochemically at time t = 0. Both curves were obtained in the absence of K^+ under virtually identical conditions. The dashed line represents a simulation of these experiments using the parameter set of Table V.

observation has been reported by Pratap, Robinson, and Steinberg (1991). They have interpreted it as the release of the first Na^+ ion (RH 421 signal) before the conformational change occurs (5-IAF signal). However, it should be noted that both fluorescence signals can be fitted much better by two exponentials than by one. The faster process is the major component in both experiments and has almost the same time constant, τ, of ~60 ms ($t_{1/2}$ = 42 ms). The slower component is significantly different in sign and amplitude. It might depend on unspecific effects which have to be attributed to the dyes (unpublished data).

Experiments with cardiotonic steroids. Another method to determine the rate constants of Na^+ release is based on experiments with cardiotonic steroids (CS). CS are known to be specific inhibitors of the Na,K-pump. Inhibition occurs when one molecule is bound per αβ protomer. The binding may be described by a single reversible equilibrium (Baker and Willis, 1970; Erdmann and Schoner, 1973; Askari,

Kakar, and Huang, 1988). Recently published data show that the use of CS allows discrimination between two distinct electrogenic steps in the reaction sequence $(Na_3)\cdot E_1\text{-}P \leftrightarrow P\text{-}E_2\cdot(Na_2)$ and $P\text{-}E_2\cdot(Na_2) \leftrightarrow P\text{-}E_2$ (Stürmer and Apell, 1992). This observation stimulated the following experiments.

In a first series of experiments, RH 421-labeled membrane fragments were phosphorylated by ATP in a buffer containing 100 mM Na^+ in the absence of K^+ and in the presence of various concentrations of strophanthidin. Some of the experiments are shown in Fig. 10. The kinetics have been accelerated by use of the aglycone strophanthidin instead of the glycoside ouabain. The rate constants for association and dissociation of the cardiac aglycones are higher than the rates of the correspond-

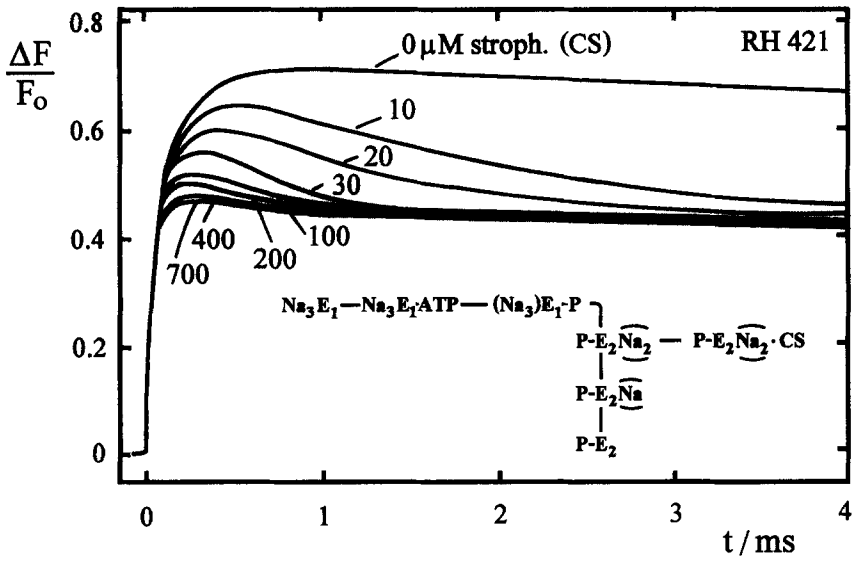

FIGURE 10. Time course of the relative fluorescence change $\Delta F(t)/F_0$ of RH 421-labeled membrane fragments after phosphorylation by ATP in the presence of 100 mM NaCl, 25 mM histidine, 0.5 mM EDTA, 10 mM $MgCl_2$, 20 μM cg-ATP and the indicated concentration of strophanthidin. About 4 μM ATP were released photochemically at time $t = 0$. The temperature was 20°C. The curves have been obtained in the nominal absence of K^+.

ing glycosides. However, the binding affinity is reduced compared to their corresponding glycosides (Yoda and Yoda, 1976). These experiments were based on the finding that up to 1 mM strophanthidin does not bind significantly to the enzyme in the presence of 100 mM NaCl before it is phosphorylated by ATP (data not shown). Upon phosphorylation the enzyme undergoes a conformational transition to the phosphorylated states of E_2 and binds almost quantitatively one strophanthidin molecule per α-subunit (Erdmann and Schoner, 1973; Askari et al., 1988). In the presence of 100 mM Na^+ and in the absence of strophanthidin the steady state fluorescence amplitude is produced mainly by states $P\text{-}E_2\cdot(Na)$ and $P\text{-}E_2$ (Table I). In the presence of strophanthidin the final state will be a $P\text{-}E_2\cdot(Na_2)$-strophanthidin complex. Since in this state 2 Na^+ ions are trapped inside the protein dielectric

(Jørgensen and Andersen, 1988; Stürmer and Apell, 1992), the final fluorescence amplitude is lower than in the absence of strophanthidin (Fig. 10).

Both, in the absence and in the presence of a high concentration of strophanthidin, an approximately monophasic fluorescence increase with a similar time course was observed (Fig. 10). At intermediate strophanthidin concentrations, the fluorescence signal reached a maximum and thereafter decreased towards a level corresponding to the state $P\text{-}E_2(Na_2)$. At low concentrations of strophanthidin (1–40 μM) the rate of enzyme inhibition was approximately proportional to the strophanthidin concentration (data not shown). At high strophanthidin concentrations an almost monoexponential fluorescence increase (~45%) has been observed. The time constant of the RH 421 signal was similar in the absence and in the presence of a high concentration of strophanthidin ($t_{1/2} \cong 40$ ms).

The effect of strophanthidin on the fluorescence of the 5-IAF-labeled membrane fragments was investigated using two approaches: (*a*) Addition of strophanthidin to the phosphorylated enzyme: in a first series of experiments, 5-IAF-labeled membrane

TABLE I

Distribution (in Percent) Between Different States of the Phosphoenzyme in Various Na^+ Concentrations

Na/mM	$(Na_3)\cdot E_1\text{-}P$	$P\text{-}E_2\cdot Na_2$	$P\text{-}E_2\cdot Na$	$P\text{-}E_2$
20	3.0	0.18	15.9	79.7
40	3.0	0.6	27.5	68.8
100	4.9	2.5	46.9	46.9
200	13.1	5.8	54.2	27.1
300	23.4	7.8	48.7	16.2
500	44.6	9.7	36.2	7.2
700	57.8	9.3	24.9	3.6
1000	71.7	8.3	15.5	1.5

The values were calculated according to the Post-Albers-scheme of Fig. 3 using the parameters given in Table V.

fragments were phosphorylated by ATP in a buffer which contained 40 mM Na^+ and 0 K^+. This caused a fluorescence decrease of 3% (Stürmer et al., 1989). In 40 mM Na^+ more than 90% of the phosphorylated enzyme is expected to be in states $P\text{-}E_2\cdot(Na)$ and $P\text{-}E_2$ (see Table I). When various concentrations of strophanthidin were then added to the phosphorylated enzyme to induce the transition $P\text{-}E_2 \rightarrow \ldots \rightarrow P\text{-}E_2\cdot(Na_2)\cdot CS$, only a small further decrease (0.2%) of the 5-IAF fluorescence was observed. This minor decrease is presumably produced, when that part of the enzyme, which is still in the state $(Na_3)E_1\text{-}P$ (less than 5%, Table I), advances into the inhibited state $P\text{-}E_2(Na_2)\cdot CS$. These findings support the idea that the transition $(Na_3)\cdot E_1\text{-}P \rightarrow P\text{-}E_2\cdot(Na)_2$ is detected by the 5-IAF label.

To prove this, the experiments were repeated in 2 M NaCl. In this case the phosphorylated enzyme may be expected to remain mainly in the state $(Na_3)\cdot E_1\text{-}P$, and indeed, upon addition of ATP the 5-IAF fluorescence stayed constant besides a small unspecific effect (Fig. 11). When under this condition CS was added to the phosphorylated enzyme, it underwent a conformational transition and proceeded

into the state $P\text{-}E_2\cdot(Na_2)\cdot CS$ (Fig. 11). In the presence of strophanthidin the pump is completely inhibited and the observed maximum fluorescence decrease of ~7.5% is equal to the decrease, which is observed for the reaction sequence $(Na_3)E_1 \rightarrow \ldots \rightarrow P\text{-}E_2$. This observation supports the hypothesis that 5-IAF indeed monitors the conformational transition $(Na_3)\cdot E_1\text{-}P \rightarrow P\text{-}E_2\cdot(Na_2)$. It should be noted that the relative fluorescence changes of the 5-IAF-labeled membrane fragments are dependent on ionic strength and are generally 2–3 times larger in buffers of high ionic strength compared to an ionic strength of 200 mM (pH 7.2).

(*b*) Enzyme phosphorylation in the presence of strophanthidin: 5-IAF-labeled membrane fragments were incubated with NaCl (40–200 mM), 25 mM histidine, 0.5 mM EDTA, 10 mM $MgCl_2$, 50 μM cg-ATP and with various concentrations of strophanthidin. At time $t = 0$, ~10 μM ATP were released by a light flash (data not shown). The final level of the 5-IAF fluorescence after phosphorylation was the same in the absence and in the presence of strophanthidin. In the absence of CS the

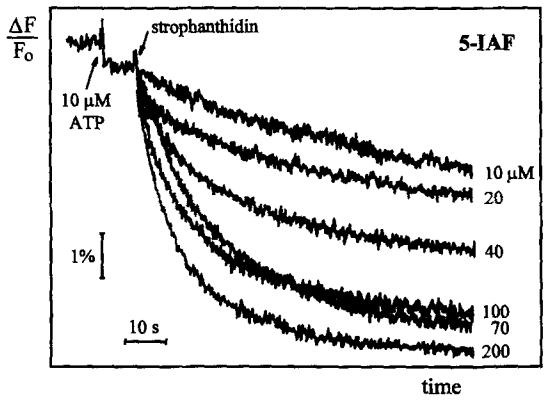

FIGURE 11. Strophanthidin induced fluorescence change $\Delta F(t)/F_o$ of 5-IAF-labeled membrane fragments in the presence of 2 M NaCl, 25 mM histidine, 0.5 mM EDTA, 10 mM $MgCl_2$ and 10 μM ATP. Strophanthidin was added after phosphorylation by ATP to obtain the indicated final concentration. The small ATP-induced effect is an artifact, since it can be observed also in the absence of Mg^{2+}, when no phosphorylation occurs. The temperature was 20°C.

enzyme is distributed between the different phosphorylated states of E_2, in the presence of CS it is locked in state $P\text{-}E_2\cdot(Na_2)\cdot CS$. The missing sensitivity against different phosphorylated states of E_2 supports the idea that the 5-IAF-fluorescence label monitors only the conformational transition $(Na_3)\cdot E_1\text{-}P \leftrightarrow (Na_2)\cdot E_2\text{-}P$. Enzyme phosphorylation in buffer containing 2 M NaCl and strophanthidin produced a fluorescence decrease comparable to the effect presented in Fig. 11 (data not shown).

Comparison of Electric and Optical Signals

Changes of transient electric currents, which result from charge movement within the membrane dielectric, contain information on the dielectric contributions of individual steps in the reaction sequence $(Na_3)\cdot E_1\text{-}P \leftrightarrow P\text{-}E_2\cdot(Na_2) \leftrightarrow P\text{-}E_2$. Membrane fragments were adsorbed to the lipid bilayer in the presence of 250 μM cg-ATP, Mg^{2+} ions and various concentrations of Na^+ in the aqueous phase. A transient electric current was initiated when ~30 μM ATP were liberated from cg-ATP by a

light flash. The intrinsic pump current, $I_p(t)$, can be evaluated from the current signal, $I(t)$, picked up in the external measuring circuit (Borlinghaus et al., 1987). To analyze quantitatively the current transients in terms of our model, it is necessary to assign dielectric coefficients to the electrogenic reaction steps (Läuger and Apell, 1986): β for the transition $(Na_3)\cdot E_1\text{-}P \leftrightarrow P\text{-}E_2\cdot(Na_2)$, δ_1 for $P\text{-}E_2\cdot(Na_2) \leftrightarrow P\text{-}E_2\cdot(Na)$, and δ_2 for $P\text{-}E_2\cdot(Na) \leftrightarrow P\text{-}E_2$. Assuming that at time $t = 0$, all enzyme is in state $Na_3\cdot E_1$ the charge movement $Q(t)$, which is associated with this reaction sequence can be written as:

$$Q(t) = q_\beta(t) + q_{\delta 1}(t) + q_{\delta 2}(t). \tag{8}$$

q_β accounts for the charge, which is moved with the conformational transition $(Na_3)\cdot E_1\text{-}P \leftrightarrow P\text{-}E_2\cdot(Na_2)$. $q_{\delta 1}$ and $q_{\delta 2}$ account for the charge movement during the release of the two ions from state $P\text{-}E_2\cdot(Na_2)$. Enzyme phosphorylation and binding of strophanthidin to state $P\text{-}E_2\cdot(Na_2)$ have been shown to be electroneutral (Borlinghaus et al., 1987).

The relative contribution of each individual term in Eq. 8 depends on the Na^+ concentration. At low Na^+ concentrations (<100 mM) and in the absence of strophanthidin, most of the enzyme proceeds to state $P\text{-}E_2$ after phosphorylation and all terms of Eq. 8 will contribute to the signal observed in the electric experiment: $Q_{(-CS)}(t \to \infty) = q_\beta(t \to \infty) + q_{\delta 1}(t \to \infty) + q_{\delta 2}(t \to \infty)$.

In the presence of 1 mM strophanthidin, the phosphorylated enzyme ends up completely in state $P\text{-}E_2\cdot(Na_2)\cdot CS$. Then the equation $Q_{(+CS)}(t \to \infty) = q_\beta$ will hold. The ratio, S, of charge transferred in the absence and in the presence of 1 mM strophanthidin in a low concentration of Na^+ may be used as a measure for the relative contributions of the two electrogenic steps which are associated with Na^+ release at the extracellular face of the pump.

$$S \equiv \frac{Q_{(-CS)}\,(t \to \infty)}{Q_{(+CS)}\,(t \to \infty)} = \frac{q_\beta + q_{\delta 1} + q_{\delta 2}}{q_\beta}. \tag{9}$$

The second part of the equation holds only for low Na^+ concentrations, when the steady state after phosphorylation is $P\text{-}E_2$ in the absence of CS and $P\text{-}E_2(Na_2)CS$ in the presence of CS. Then the ratio S can be used to determine the ratio of the dielectric coefficients $(\delta_1 + \delta_2)$ and β by extrapolation to low Na^+ concentrations where the population of state $(Na_3)\cdot E_1\text{-}P$ approaches zero.

$$\frac{\delta_1 + \delta_2}{\beta} = S - 1. \tag{10}$$

With increasing Na^+ concentration (>500 mM) $Q_{(-CS)}$ becomes smaller because less enzyme proceeds further than state $(Na_3)\cdot E_1\text{-}P$. Under this condition the relation $Q_{(-CS)} < Q_{(+CS)}$ holds, because $Q_{(+CS)}$ remains constant for all Na^+ concentrations.

The amount of pumped charge, Q, has been obtained by integration of the transient pump current, $I_p(t)$, which was measured in the absence and in the presence of 1 mM strophanthidin. In an Na^+ concentration of 150 mM, the amplitudes and the time courses of the transient currents obtained in the absence and in the presence of 1 mM strophanthidin did not differ significantly (Fig. 12).

Control experiments have been performed to make sure that the applied concen-

tration of strophanthidin was sufficient to block all ion pumps. (*a*) In the absence of strophanthidin a small quasi-stationary current, I_p^∞, has been observed (Fendler et al., 1985; Borlinghaus et al., 1987; Apell, Borlinghaus, and Läuger, 1987). In the presence of strophanthidin no I_p^∞ has been observed. (*b*) It is known from the literature (Borlinghaus et al., 1987) that a second light flash applied a short period (0.5-2.5 s) after the first flash elicits a second but smaller current transient due to the amount of pumps which returned into state Na_3E_1. After addition of strophanthidin we found that for times $t \geq 1$ s the second transient had vanished completely (data not shown). (*c*) The density of active pumps in the membrane fragments has been reduced by UV inactivation with increasing doses of light (λ = 308 nm) from an excimer laser until the remaining enzymatic activity was 10%. Compared to experiments with fully active protein only the current amplitude was strongly reduced. Because the kinetics of the transient and of the inhibition was unaffected, it can be concluded that binding of strophanthidin to the pump was not limited by a reduced local concentrations in the gap between membrane fragments and bilayer.

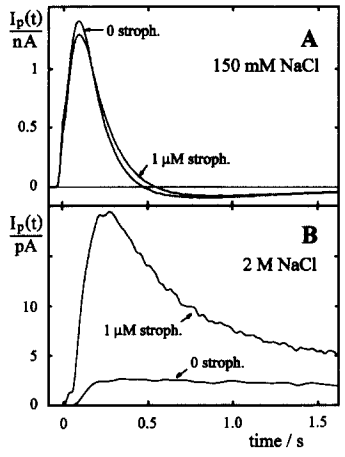

FIGURE 12. Current transients in the absence of K^+ after enzyme phosphorylation at time t = 0. The aqueous solutions contained 150 mM NaCl (*A*) and 2 M NaCl (*B*), 30 mM imidazole, 1 mM EDTA, 10 mM $MgCl_2$, pH 7.2, 250 µM cg-ATP and 0 or 1 mM strophanthidin (*Stroph.*). About 30 µM ATP were released from cg-ATP. The Na,K-ATPase membrane fragments were added to the *cis* compartment 40 min, and the strophanthidin 10 min before the corresponding experiment.

Experiments with 5-IAF and RH 421-labeled membrane fragments indicated that at a Na^+ concentration of 2 M addition of strophanthidin to the phosphorylated enzyme induces the conformational transition $(Na_3)\cdot E_1\text{-}P \rightarrow P\text{-}E_2\cdot(Na_2)$ (see above). To compare these optical experiments with bilayer experiments, we determined transient electric currents in 2 M NaCl in the absence and presence of strophanthidin. Data are shown in Fig. 12 *B*. The sign of the current transients corresponds to a translocation of positive charge towards the extracellular face of the membrane fragments. In the absence of strophanthidin the amount of translocated charge, as calculated from the current transient, was reduced by more than 10-fold in 2 M NaCl compared with the charge obtained in 150 mM NaCl. In optical experiments, which were performed under virtually identical conditions the steady state fluorescence amplitude changed only negligibly upon phosphorylation (Stürmer and Apell, 1992). Both experiments indicate that the phosphorylated enzyme, obtained in 2 M NaCl, will be almost quantitatively in state $(Na_3)\cdot E_1\text{-}P$. The time course of the current transient in 2 M NaCl was significantly slower than in 150 mM NaCl. This is in

accordance with findings from optical experiments in high ionic strength (see previous section).

Comparing the electric current transients obtained at a Na concentration of 2 M in the absence and in the presence of 1 mM strophanthidin (Fig. 12 *B*), averaged over all experiments a sevenfold increase of the amplitude of the current transient can be observed after addition of 1 mM strophanthidin. The additional charge, which has moved in the presence of strophanthidin, is most likely due to the transition $(Na_3)\cdot E_1\text{-}P \rightarrow P\text{-}E_2\cdot(Na_2)$ and the transition into the inhibited state $P\text{-}E_2\cdot(Na_2)\cdot CS$. The finding that in 2 M NaCl the strophanthidin-induced current transient has vanished within 8 s and has transferred approximately the same amount of charge as determined in buffer containing 150 mM Na^+ and no strophanthidin, is another argument against objections that strophanthidin binding may be incomplete.

In contrast to the well reproduced time courses of the currents, the amplitudes are known to vary up to twofold between experiments with different bilayers (Borlinghaus et al., 1987). To circumvent the effect of amplitude variation the following series of experiments have been performed. A first current transient has been measured in the absence of strophanthidin and used to calculate the transferred charge $Q_{(-CS)}$. Thereafter, 1 mM strophanthidin has been added and equilibrated for 10 min before the measurement of a second current transient. The corresponding charge transferred in the pump was $Q_{(+CS)}$. In this way the ratio of charges $S \equiv Q_{(-CS)}/Q_{(+CS)}$ has been obtained with the identical enzyme lipid bilayer system. This procedure allowed a precise estimate of the dielectric contributions of the different electrogenic steps at Na^+ concentrations between 50 mM and 2.2 M. The experimentally determined ratio S is plotted in Fig. 13. The inactivation of the pump by strophanthidin in absence of ATP is prevented in Na^+ concentrations above 50 mM, as has been checked by measurements of the enzymatic activity.

Fluorescence Signals Associated with Release of Na^+ and Binding of K^+ at the Extracellular Side

When ATP is released from cg-ATP in the presence of Na^+ and K^+ ions, the reaction sequence $Na_3\cdot E_1 \rightarrow Na_3\cdot E_1\cdot ATP \rightarrow (Na_3)\cdot E_1\text{-}P \rightarrow P\text{-}E_2\cdot(Na_2) \rightarrow P\text{-}E_2 \rightarrow P\text{-}E_2\cdot(K_2) \rightarrow E_2\cdot(K_2)$ is triggered. The enzyme remains essentially in state $E_2\cdot(K_2)$, if the concentration of ATP is much smaller than the apparent dissociation constant of the low-affinity ATP binding site, which has been determined to be between 8 μM (see below) and 13 μM (Apell, Häring, and Roudna, 1990) in rabbit kidney enzyme.

In Fig. 14 *A*, the time course of the RH 421 fluorescence is shown in the presence of 150 mM Na^+ and various concentrations of K^+. After phosphorylation of the enzyme by ATP and in the absence of K^+ an approximately monoexponential fluorescence increase of ~70% has been observed. This fluorescence change reflects the transition $Na_3\cdot E_1 \rightarrow (Na_3)\cdot E_1\text{-}P \rightarrow P\text{-}E_2\cdot(Na_2) \rightarrow P\text{-}E_2$. In the presence of 5 mM K^+, the additional subsequent reaction sequence $P\text{-}E_2 \rightarrow E_2\cdot(K_2)$ has been initiated. Since state $E_2\cdot(K_2)$ has a lower fluorescence than state $P\text{-}E_2$ (Stürmer et al., 1991*b*), a fluorescence increase of only 20% was found. In 5 mM K^+ the transition $P\text{-}E_2 \rightarrow E_2\cdot(K_2)$ is fast compared to the conformational change $(Na_3)\cdot E_1\text{-}P \rightarrow P\text{-}E_2\cdot(Na_2)$. Thus, a monophasic fluorescence increase resulted. In the absence of K^+, the time $t_{1/2}$ for half-maximal signal amplitudes was ~40 ms, in the presence of 5 mM K^+, the

half maximal signal amplitude was reached at $t_{1/2} \approx 30$ ms. In Fig. 14 *B*, the same experiments have been performed in the presence of the 5-IAF fluorescence label. In the absence of K^+, enzyme phosphorylation induces a fluorescence decrease of ~2.5%. In the presence of 5 K^+ mM the fluorescence amplitude dropped ~10%. The larger fluorescence decrease in the presence of K^+ is due to the fact that state $E_2 \cdot (K_2)$ has a lower fluorescence than state $P\text{-}E_2$ (Kapakos and Steinberg, 1986; Stürmer et al., 1989). At 0 mM K^+ and at 5 mM K^+, the time constant for both signals is almost the same (~60 ms). At intermediate K^+ concentrations, the

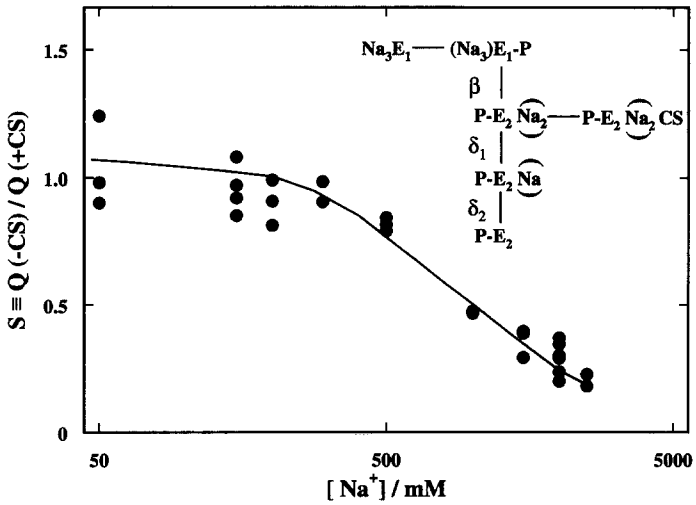

FIGURE 13. Dependence of $S \equiv Q_{(-CS)}/Q_{(+CS)} = (q_{\delta 1} + q_{\delta 2} + q_\beta)/q_\beta$ on Na^+ concentration. $Q_{(+CS)}$ is defined as the charge transferred in the presence of cardiotonic steroids; $Q_{(-CS)}$ is the charge, which is transferred in the absence of *CS*. After adsorption of the membrane fragments to the black lipid bilayer two or three current transients were recorded. Then 1 mM strophanthidin was added to the solution containing the membrane fragments. After an equilibration time of 10 min, a further current transient was recorded. The aqueous solution contained 30 mM imidazole, 1 mM EDTA, 10 mM $MgCl_2$, 250 μM cg-ATP, 0.02 U of apyrase to remove traces of ATP and the indicated concentrations of NaCl and strophanthidin. At $t = 0$, ATP was released from cg-ATP. All signals were recorded at $T = 20$°C. The current transients were integrated for the first second after ATP release and the total translocated charge was determined. The line represents the numerical simulation using the parameters given in Table V and the dielectric coefficients given in the text.

half-time $t_{1/2}$ increases, because the kinetics of K^+ binding will in part become rate limiting (Stürmer et al., 1989).

The half-saturating concentration of extracellular K^+ binding, K_M, can be determined from similar experiments as shown in Fig. 14 *A*, in which the time course of the RH fluorescence has been recorded over a period of 6 s to determine the stationary fluorescence amplitude. Increasing amounts of K^+ in the buffer reduced the steady state level of the RH 421 signal as in Fig. 14 *A*. When the differences of the steady state fluorescence between no K^+ and a given concentration are plotted

against K^+ concentration, a titration curve of Michaelis-Menten type is obtained. The determined values of K_m depended on Na^+ and ATP concentration as shown in Table II.

To be able to compare more carefully the ability of the numerical model of the pump cycle, the interdependence of Na^+ and K^+ concentration on the time course and amplitude of the RH 421 signals has been determined for a series of different ionic conditions. The fluorescence signals can be characterized by two parameters, by the steady state level of fluorescence, $\Delta F/F_0$, and by the half-time for fluorescence change, $t_{1/2}$, of the fluorescence signal. The experimental results as well as the results of the numerical simulation, which is discussed later, are collected in Table III.

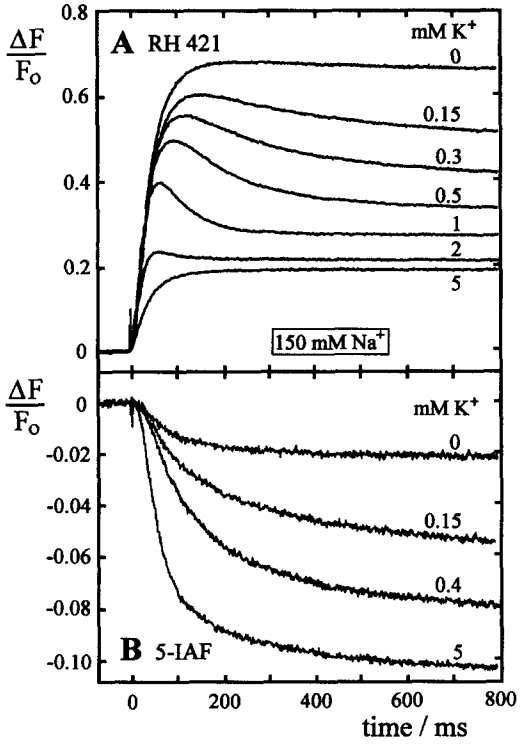

FIGURE 14. Time course of fluorescence changes of (*A*) RH 421 or (*B*) 5-IAF-labeled membrane fragments. Membrane fragments were equilibrated in the presence of 150 mM NaCl, 25 mM histidine, 0.5 mM EDTA, 10 mM $MgCl_2$ and 20 μM cg-ATP. At time $t = 0$, ATP was released from cg-ATP. This induces enzyme phosphorylation and a conformational transition to state P-E_2. In the presence of K^+, the reaction proceeds by K^+ binding, occlusion of K^+ and enzyme dephosphorylation. Because the ATP concentration is below the affinity of the low-affinity ATP-binding side, the enzyme will end up essentially in state $E_2(K_2)$. The temperature was 20°C.

Fluorescence experiments with cardiotonic steroids. According to the proposed mechanism, the kinetics of inhibition by CS depends on the population of state $P\text{-}E_2(Na_2)$. Therefore, experiments were carried out, in which the population of that state was varied by various concentrations of K^+ in the buffer. The time course of the signal can be used to obtain information on Na^+ and K^+ binding rates. In Fig. 15 ATP-concentration jump experiments are presented which were performed in buffer containing 200 mM NaCl, 4 or 20 mM KCl, 25 mM histidine, 0.5 mM EDTA, 10 mM $MgCl_2$, 20 μM cg-ATP and various concentrations of strophanthidin. The high concentration of Na^+ prevented an inhibition of unphosphorylated enzyme. In the presence of 4 mM K^+ the fluorescence signals diverge immediately after the release

TABLE II

Dependence of the Half-saturating Concentration of K^+ Binding, K_M, on Na^+ and ATP Concentration

ATP/μM	Na/mM		
	40	100	200
		μM	
4	80 (75) μM	140 (130)	210 (175) μM
10		180 (200)	
50		245 (345)	
500		630 (600)	

The experimental determined K_M values were determined by linear regression from Eadie-Hoffstee plots with correlation coefficients better than 0.99. The numbers in parentheses were obtained by numerical simulation of the reaction cycle.

of ATP (Fig. 15 *A*). When repeated in the presence of 20 mM K^+ (Fig. 15 *B*), the fluorescence traces diverge only after times longer than 1 s.

As a control RH 421-labeled membrane fragments were added to a buffer containing 200 mM Na^+, 4 or 20 mM K^+, 25 mM histidine 0.5 mM EDTA, 10 mM $MgCl_2$ and 4 μM ATP. The fluorescence stabilized at a level which corresponds to state $E_2(K_2)$. Subsequent addition of 700 μM strophanthidin led to an increase of the fluorescence by 15% (data not shown). This is consistent with the results presented in Fig. 15.

Inhibition of enzymatic activity by strophanthidin at various potassium concentrations. Information concerning the rates of ion release and binding on the extracellular side can be obtained from experiments in which the inhibition of enzymatic activity by strophanthidin in state $P\text{-}E_2\cdot(Na_2)$ was studied at various K^+ concentrations. These experiments are based on the idea that under turnover conditions the amount of enzyme in state $P\text{-}E_2\cdot(Na_2)$ depends on the rate constant of the rate limiting step of the reaction sequence $P\text{-}E_2\cdot(Na_2) \rightarrow P\text{-}E_2 \rightarrow P\text{-}E_2\cdot(K_2) \rightarrow E_2\cdot(K_2)$. If the transition $P\text{-}E_2\cdot(Na_2) \rightarrow P\text{-}E_2$ is assumed to be slow compared to the subsequent K^+ binding steps $P\text{-}E_2 \rightarrow E_2\cdot(K_2)$, the apparent strophanthidin affinity may be expected to be not

TABLE III

Time Dependence of RH 421 Fluorescence upon Photolysis of cg-ATP in the Presence of Na^+ and K^+

c[K^+]	[Na^+] = 40 mM		[Na^+] = 100 mM		[Na^+] = 200 mM	
	$t_{1/2}$	$-\Delta F/F_0$	$t_{1/2}$	$-\Delta F/F_0$	$t_{1/2}$	$-\Delta F/F_0$
μM	*ms*	%	*ms*	%	*ms*	%
50	350 (272)	12.1 (15.3)	320 (322)	5.9 (11.1)	317 (380)	4.2 (6.0)
100	223 (186)	18.9 (21.0)	270 (238)	14 (16.3)	275 (299)	12.8 (9.6)
200	122 (113)	26.2 (25.2)	180 (147)	20 (21.0)	272 (208)	16.1 (13.6)
300	89 (82)	28.5 (27.6)	127 (113)	24.8 (23.3)	198 (159)	21.5 (15.8)
500	63 (53)	30.6 (29.5)	79 (72.5)	28.2 (25.6)	124 (109)	24.3 (18.2)

The decay of the fluorescence transient could be described by a single exponential. $t_{1/2}$ has been calculated by linear regression to the logarithm of the data with correlation coefficients better than 0.99. The numbers in the parentheses were obtained by numerical simulation of the reaction cycle.

significantly affected by the K^+ concentration. If, on the other hand, the step $P\text{-}E_2\cdot(Na_2) \leftrightarrow P\text{-}E_2$ is fast and reversible, the apparent strophanthidin affinity should be affected by K^+. Therefore, the enzymatic activity has been measured in buffer which contained 100 mM NaCl, 10 mM $MgCl_2$, 1 mM ATP and various K^+ concentrations between 0 and 90 mM. Aliquots of strophanthidin have been added successively and for each concentration the corresponding activity has been determined. The resulting strophanthidin titration curves have been used to calculate the concentration of half maximal inhibition, K_M. In Fig. 16, K_M is plotted against the K^+ concentration. Correspondingly the reaction flux into the inhibited state $P\text{-}E_2\cdot(Na_2)\cdot CS$ could be modulated by K^+ concentration and produced a K^+-dependent binding kinetics (Fig. 16, *inset*). A method independent of the RH 421

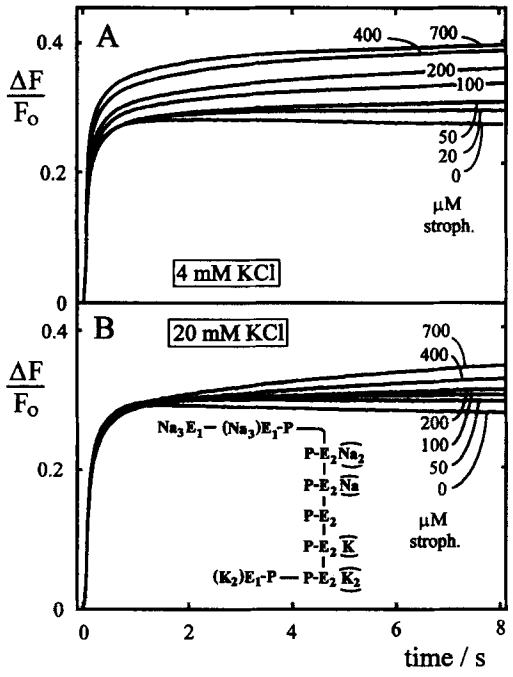

FIGURE 15. Effect of strophanthidin on the time course of RH 421-labeled membrane fragments. The membrane fragments were incubated in a buffer containing 200 mM NaCl, 25 mM histidine 0.5 mM EDTA, 10 mM $MgCl_2$, 20 μM cg-ATP and the indicated concentration of strophanthidin and 4 mM KCl (*A*) or 20 mM KCl (*B*). After ATP release, a fluorescence increase can be observed. In the absence of strophanthidin, the enzyme will end up in state $E_2(K_2)$. In the presence of 700 μM strophanthidin, a major part of the enzyme will be found in states $P\text{-}E_2(Na_2)\cdot CS$ and/or $P\text{-}E_2(K_2)\cdot CS$. Because states $P\text{-}E_2(Na_2)\cdot CS$ and/or $P\text{-}E_2(K_2)\cdot CS$ have a higher fluorescence than state $E_2(K_2)$, the fluorescence at 700 μM strophanthidin is higher. All experiments were performed at a temperature of 20°C.

experiments, which led to similar results, was the detection of anthroylouabain (AO) binding. This compound is a fluorescent member of the family of cardiac steroids, which increases its fluorescence, when it binds to the Na,K-ATPase (Fortes, 1986). AO binding was initiated by addition of 0.5 mM ATP to a solution containing 10 μg/ml membrane fragments, 20 μM AO, 25 mM histidine, 0.5 mM EDTA, 100 mM NaCl, 10 mM $MgCl_2$, and a given concentration of K^+. The fluorescence increase could be fitted by a single exponential from which rate constants can be calculated. Increasing the K^+ concentration from 0 to 1 mM reduced the apparent binding constant by a factor of 4 (Table IV).

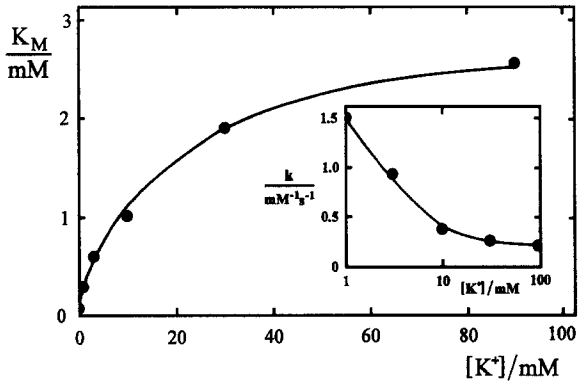

FIGURE 16. Dependence of the apparent strophanthidin affinity on K^+ concentration. The enzymatic activity has been measured by the pyruvate-kinase/lactate-dehydrogenase assay in buffers of 100 mM NaCl, 10 mM $MgCl_2$, 1 mM ATP, the indicated K^+ concentration and various concentrations of strophanthidin. From these data the strophanthidin concentration that produced half-maximal enzyme inhibition has been determined (*circles*). The line represents the result of the numerical simulation. (*Inset*) Dependence of the rate of strophanthidin binding (and enzyme inhibition) on the K^+ concentration. Experimental conditions and procedure were similar to the experiment described above. The time course of strophanthidin binding could be described by a single exponential. The line was obtained by numerical simulation.

Fluorescence Changes Associated with the Conformational Transition $E_2(K_2) \rightarrow E_1$

The conformational transition $E_2(K_2) \rightarrow E_1$·ATP cannot be examined with electric methods or with the RH 421 fluorescence dye, because this transition is not electrogenic (Bahinski, Nakao, and Gadsby, 1988; Stürmer et al., 1989; Bühler et al., 1991). Therefore, the K^+ and ATP dependence of this transition was examined using 5-IAF-labeled enzyme. The following experiments made it possible to determine the rate constants of the reactions $E_2(K_2) \leftrightarrow$ ATP·$E_2(K_2)$ and ATP·$E_2(K_2) \leftrightarrow K_2E_1$·ATP.

ATP-concentration dependence: when the medium contained millimolar concentrations of K^+, but no Na^+, addition of ATP led to an increase of the fluorescence of 5-IAF-labeled membrane fragments (Stürmer et al., 1989). This increase reflects the conformational transition $E_2(K_2) \rightarrow E_1$. ATP concentration jump experiments were performed in buffer containing 1.5 mM KCl, 30 mM imidazole, 1 mM EDTA, 5 mM $MgCl_2$, ~6 μg/ml membrane fragments and the various concentration of ATP after the light flash. The signals were analyzed with respect of the maximal fluorescence amplitude and the half saturation time. The ATP-concentration dependence is shown

TABLE IV

Dependence of the Anthroylouabain Binding Rate on K^+ Concentration: Comparison of Data and Simulations

[K^+]	AO binding rate	Simulation
μM	$mM^{-1}\,s^{-1}$	$mM^{-1}\,s^{-1}$
0	1.2	1.3
100	0.85	0.89
200	0.64	0.71
300	0.6	0.6
500	0.46	0.39
1000	0.28	0.25

in Fig. 17. ATP binding to state $E_2 \cdot (K_2)$ is rate limiting in low concentrations, whereas in high ATP the conformational transition from E_2 to E_1 becomes rate limiting. From the data shown in Fig. 17, an apparent ATP affinity of 2 μM has been determined with respect to the fluorescence amplitudes. The lower panel of Fig. 17 contains the time $t_{1/2}$, which indicates the time of half maximum fluorescence change. When the reciprocal value of $t_{1/2}$ is plotted against the ATP concentration, Michaelis-Menten type kinetics can be observed. $t_{1/2}$ was 125 ms in the presence of saturating ATP. The apparent affinity of ATP was determined to be 8 μM.

K^+-concentration dependence: the K^+ dependence of the ATP-induced reaction sequence $E_2(K_2) \leftrightarrow ATP \cdot E_2(K_2) \leftrightarrow K_2E_1 \cdot ATP$ has been determined by the same type of experiments as described for the ATP-concentration dependence. The cg-ATP concentration was kept at 100 μM to obtain 20 μM free ATP upon the light flash. The K^+ concentration has been varied between 0.25 mM and 10 mM. The results are

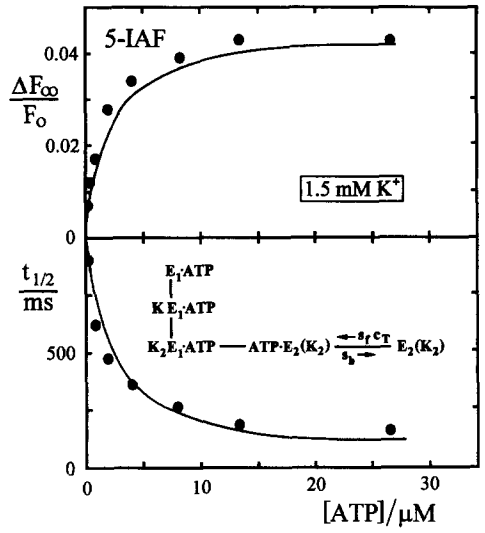

FIGURE 17. Dependence of amplitude $\Delta F_\infty/F_0$ and half time $t_{1/2}$ of the ATP-induced 5-IAF fluorescence change on ATP concentration. $t_{1/2}$ is the time at which $\Delta F(t)/F_0$ reaches its half-maximal value. The labeled enzyme was incubated in buffer containing 1.5 mM KCl, 30 mM imidazole, 1 mM EDTA, 5 mM $MgCl_2$, about 6 μg/ml membrane fragments and the indicated concentration of ATP, after it was released from cg-ATP. The temperature was 20°C. Data are represented by circles. The line has been obtained by numerical simulation of the fluorescence experiments.

shown in Fig. 18. The signal amplitude increased with increasing K^+ concentration up to a maximum at 1.5 mM K^+ and decreased towards higher concentrations (Fig. 18 *A*). The half-time $t_{1/2}$ of the fluorescence increase is shown in Fig. 18 *B*. $t_{1/2}$ decreased from 240 ms to 60 ms when the K^+ concentration is increased from 0.25 mM to 10 mM.

Enzymatic Activity of Na,K-ATPase as a Function of Na^+ and K^+ Concentration

To get further evidence for the determined rate constants and affinities of the reaction scheme, experiments from Skou (1975) have been repeated with rabbit enzyme. In these experiments the rate of ATP hydrolysis has been measured as a function of Na^+ and K^+ concentration (Fig. 19) using the pyruvate kinase/lactate dehydrogenase assay. Two features of the results should be mentioned. (*a*) The shape of the curve in our experiment is different from the curve published by Skou (1975).

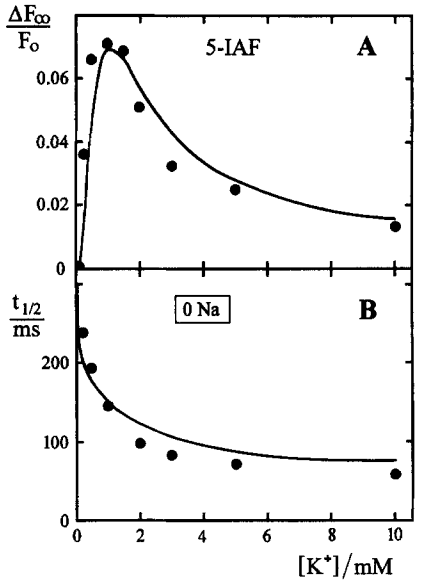

FIGURE 18. Dependence of (*A*) amplitude $\Delta F_\infty/F_o$ and (*B*) half time $t_{1/2}$ of the ATP-induced 5-IAF fluorescence on K^+ concentration. $t_{1/2}$ is the time at which $\Delta F(t)/F_o$ reaches its half-maximal value. At time $t = 0$ about 20 μM ATP were released from cg-ATP in a solution containing 30 mM imidazole, 1 mM EDTA, pH 7.2, 5 mM Mg^{2+} and the indicated concentration of KCl. Data are represented by circles. The line has been obtained by numerical simulation of the reaction cycle.

However, it should be noted that our experiments were obtained under different conditions (T = 20°C, 0 mM P_i) and the source of enzyme was different, rabbit kidney instead of ox brain. (*b*) The experimental curve obtained with our enzyme can be reproduced satisfactorily by numerical simulations. The poor agreement with the curve obtained from ox brain indicates that the rate constants of the rate limiting steps in the pump cycle have to be different for both enzyme preparations.

Numerical Simulations

The experiments described in the previous paragraphs of the Results section were performed to complete the set of kinetic parameters of Table V, which are necessary

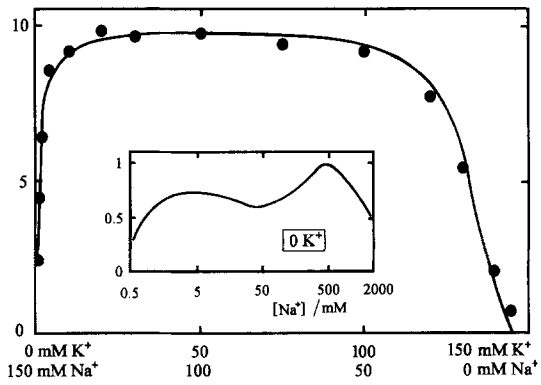

FIGURE 19. Rate of ATP hydrolysis by the Na,K-ATPase, as a function of Na^+ and K^+ concentration. The experiments were performed in a buffer containing 1 mM Tris/EDTA, 25 mM imidazole, 10 mM $MgCl_2$ and 1.5 mM ATP using the pyruvate kinase/lactate dehydrogenase assay. Experimental data are represented by circles. The line has been obtained by numerical simulation of the reaction cycle. (*Inset*) Simulation of the dependence of Na-ATPase activity on Na^+ concentration. The simulation is based on the scheme shown in Fig. 3 using the parameter set of Table V. An ATP concentration of 1 mM was assumed.

to execute the numerical simulations of the reaction model in Fig. 3. Simulations were carried out for all experiments described above without adjustment of any involved parameter of Table V. The coupled differential equations describing the extended Post-Albers cycle (Fig. 3) are presented in the Appendix. Since under some conditions, the concentrations of ATP, ADP, P_i or free cardiotonic steroids vary considerably during an experiment, these concentrations were adjusted to their actual value during the numerical simulation of the experiments. Using the set of parameters given in Table V, the measured optical and electric signals could be reproduced at least qualitatively. We did not try to obtain an optimum fit of the experimental data by adjusting the kinetic parameters, but checked instead the range of confidence of a rate constant by variation of its value to determine limits of an acceptable simulation. We carried out the analysis with a minimal number of assumptions and listed a consistent set of kinetic values describing our experiments.

Besides the kinetic parameters of the reaction cycle in Table V, an assignment of the fluorescence levels and dielectric coefficients must be made. These parameters were determined by the presented experiments or completed by values from the literature, if they have not been appointed in this paper.

Describing experiments performed with the 5-IAF method three classes of states of the pump cycle must be made with respect to the intrinsic fluorescence of the 5-IAF dye (Stürmer et al., 1989):

$$\varphi_1 \equiv f(E_1) \quad = 1: \quad \text{all states of } E_1$$

$$\varphi_2 \equiv f(P\text{-}E_2) = 0.97: \quad \text{all phosphorylated states of } E_2$$

$$\varphi_3 \equiv f(E_2(K)_2) \quad = 0.86: \quad \text{states } E_2\cdot(K_2) \text{ and ATP-}E_2\cdot(K_2).$$

The RH 421 method discriminates between states with different amount of charge bound to the enzyme:

$$\Psi_1 \equiv f(Na_3\cdot E_1) = f(Na_3\cdot E_1\cdot ATP) = f((Na_3)\cdot E_1\text{-}P) = 0.8$$

(all E_1 states with 3 Na^+ ions bound to the enzyme),

$$\Psi_2 \equiv f(Na_{0,1,2}\cdot E_1\cdot(ATP)) = f(K_{1,2}\cdot E_1\cdot(ATP)) = f(E_2(Na_2)) = f(E_2K_2) = f(E_2(K_2)\cdot ATP) = 1$$

(the remaining E_1-states and the unphosphorylated E_2-states),

$$\Psi_3 \equiv f(P\text{-}E_2\cdot(Na_2)) = f(P\text{-}E_2\cdot(K_2)) = 1.1$$

(states $P\text{-}E_2\cdot(Na_2)$ and $P\text{-}E_2\cdot(K_2)$),

$$\Psi_4 \equiv f(P\text{-}E_2(Na)) = f(P\text{-}E_2(K)) = 1.4$$

($P\text{-}E_2$ states with 1 Na^+ or 1 K^+ ions bound),

$$\Psi_5 \equiv f(P\text{-}E_2) = 1.7$$

(state $P\text{-}E_2$).

The interpretation of the electric measurements made it necessary to assign dielectric coefficients to different transitions in the reaction cycle. The analysis of the presented experiments led to the following assignments of the electrogenic steps:

TABLE V

Values of Kinetic Parameters of the Reaction Scheme of Fig. 3, Used for the Numerical Simulation of the Presented Experiments: T = 20°C

Parameter	Value	Range of confidence	Notes
K'_{Na}	3 mM	2–5 mM	Estimate from titrations on cation binding to Na,K-ATPase (Grell et al., 1991)
K'_{K}	12 mM	5–20 mM	Estimate from numerical simulations of the K^+-dependence of the transition $E_2(K_2) \rightarrow E_1$
n_{3f}	$2 \cdot 10^5$ M^{-1} s^{-1}	$> 1 \cdot 10^5$ M^{-1} s^{-1}	Estimate from the stopped flow experiments, in which we failed to resolve Na^+ binding. Phosphorylation studied indicate a value higher than 12,000 M^{-1} s^{-1} (Froehlich and Fendler, 1991).
n_{3b}	$8 \cdot 10^2$ s^{-1}	n_{3b}/n_{3f} = 4 mM	n_{3b}/n_{3f} was determined from the Na^+ dependence of RH 421 fluorescence upon cytoplasmic Na^+ binding.
a_f	$1.5 \cdot 10^7$ M^{-1} s^{-1}	$1 \cdot 10^7$ M^{-1} s^{-1} – $1 \cdot 10^8$ M^{-1} s^{-1}	From the ATP dependence of the conformational change $E_1 \rightarrow E_2$
a_b	1.64 s^{-1}	a_b/a_f = 50–200 nM	a_b was obtained from the principle of microscopic reversibility
p_f	200 s^{-1}	150–300 s^{-1}	Estimate from numerical simulations of the Na^+ dependence of the transition $E_1 \rightarrow E_2$. Mårdh and Zetterquist (1974) obtained a value of 180 s^{-1} for the pseudo-first order rate of enzyme phosphorylation.
p_b	$3.7 \cdot 10^5$ M^{-1} s^{-1}	10^3–10^6 M^{-1} s^{-1}	p_b was obtained from the principle of microscopic reversibility.
g_{3f}	22 s^{-1}	18–30 s^{-1}	Obtained from the time course of phosphorylation-induced 5-IAF and RH 421 fluorescence and from the time course of transient electric currents.
g_{3b}	180 M^{-1} s^{-1}	60–600 m^{-1} s^{-1} g_{3f}/g_{3b} = 0.12 M	Obtained from numerical simulations of the Na^+ dependence of 5-IAF and RH 421 fluorescence (see text).
g_{2f}	$\geq 5 \cdot 10^3$ s^{-1}	$3 \cdot 10^3$ s^{-1} – ?	Estimated from experiments with cardiotonic steroids (see text).
g_{2b}	$2.68 \cdot 10^3$ M^{-1} s^{-1}	g_{2f}/g_b = 1–2.5 M	Obtained from numerical simulations of the Na^+ dependence of 5-IAF and RH 421 fluorescence (see text).
g_{1f}	$\geq 1 \cdot 10^4$ s^{-1}	$5 \cdot 10^3$ s^{-1} – ?	Estimated from experiments with cardiotonic steroids (see text).
g_{1b}	$1 \cdot 10^6$ $M^{-1}s^{-1}$	g_{1f}/g_{1h} = 0.05–0.2M	Obtained from numerical simulations of the Na^+ dependence of 5-IAF and RH 421 fluorescence (see text).
m_{1f}	$3.4 \cdot 10^4$ M^{-1} s^{-1}	$2.0 \cdot 10^4$ M^{-1} s^{-1} – $5 \cdot 10^4$ M^{-1} s^{-1}	Obtained from 5-IAF and RH 421 fluorescence experiments on K^+ binding to the phosphorylated enzyme.
m_{1b}	$1 \cdot 10^1$ s^{-1}	5 s^{-1}–20 s^{-1}	Estimate from experiments on ^{86}Rb release of the phosphorylated enzyme (Forbush, 1987*b*).
m_{2f}	$5 \cdot 10^6$ M^{-1} s^{-1}	$\geq 1 \cdot 10^5$ M^{-1} s^{-1}	Estimated from the finding that the time course of RH 421 and 5-IAF fluorescence change, which was inducted by K^+ binding to the phosphoenzyme, can be fitted with a single exponential.
m_{2b}	$2 \cdot 10^3$ s^{-1}	m_{2b}/m_{2f} = 100 μM – 1 mM	

TABLE V (*continued*)

Values of Kinetic Parameters of the Reaction Scheme of Fig. 3, Used for the Numerical Simulation of the Presented Experiments: T = 20°C

Parameter	Value	Range of confidence	Notes
q_f	$1 \cdot 10^5$ s^{-1}	$\geq 1{,}000$ s^{-1}	Estimated from RH 421 fluorescence experiments with cardiotonic steroids (see text). Forbush (1988) concluded that q_f is much larger than 100 s^{-1}.
q_b	$5 \cdot 10^6$ M^{-1} s^{-1}	$\geq 1 \cdot 10^5$ M^{-1} s^{-1}	Estimate from numerical simulations of experiments on ^{86}Rb release (Forbush, 1987*b*)
s_f	$5 \cdot 10^5$ M^{-1} s^{-1}	$2.5 \cdot 10^5$ M^{-1} s^{-1} – $1 \cdot 10^6$ M^{-1} s^{-1}	Determined by numerical simulations of the ATP dependence of the 5-IAF fluorescence change which reflects the conformational transition $E_2(K_2) \rightarrow E_1$
s_b	4 s^{-1}	s_b/s_f = 4–10 μM	See above.
k_f	22 s^{-1}	15 s^{-1}–30 s^{-1}	Determined by numerical simulations of 5-IAF fluorescence experiments performed in the presence of K^+ and in the absence of Na^+
k_b	$4 \cdot 10^2$ s^{-1}	100 s^{-1}–1,000 s^{-1}	See above.
h_f	0.1 s^{-1}	$0.5 \cdot 10^{-2}$ s^{-1} – 0.5 s^{-1}	Estimated from simulations of experiments of ATP-hydrolysis of Na,K-ATPase performed at very low ATP concentration. From experiments on spontaneous ^{86}Rb deocclusion, rates of 0.1–0.3 s^{-1} have been estimated (Glynn and Richards, 1982; Forbush, 1987*b*).
h_b	$1 \cdot 10^2$ s^{-1}	50 s^{-1}–500 s^{-1}	From optical determinations of rates of conformational transition, Karlish (1980) obtained a value of 300 s^{-1}.
r_f	$8 \cdot 10^{-1}$ s^{-1}	0.3 s^{-1}–1·s^{1}	Estimated from simulations of Na-ATPase activity at very low Na^+ concentrations.
r_b	$3.3 \cdot 10^3$ M^{-1} s^{-1}	$1.\cdot 10^2$ M^{-1} s^{1} – $5 \cdot 10^4$ M^{-1} s^{-1}	r_b was obtained from the principle of microscopic reversibility
d_f	$1.0 \cdot 10^1$ s^{-1}	3 s^{-1}–30 s^{-1}	Estimated from simulations of Na-ATPase activity at higher Na concentrations.
d_b	$2.52 \cdot 10^4$ M^{-1} s^{-1}		d_b was obtained from the principle of microscopic reversibility
e_f	$0.5 \cdot 10^2$ s^{-1}	≥ 10 s^{-1}	e_f is assumed to be faster than d_f to ensure that occlusion of 2 Na^+ ions is negligible.
e_b	$1 \cdot 10^{-1}$ s^{-1}	≤ 1 s^{-1}	e_f/e_b is assumed to be larger than 10 s^{-1} to ensure that occlusion of 2 Na^+ ions is negligible.
o_f	$2 \cdot 10^6$ M^{-1} s^{-1}	$1 \cdot 10^6$ M^{-1}s^{-1} – $4 \cdot 10^6$ M^{-1} s^{-1}	Value describing the binding of strophanthidin to the phosphoenzyme. The value for anthroylouabin is ~50 times smaller.
o_b	$1 \cdot 10^{-2}$ s^{-1}	$0.5 \cdot 10^{-2}$s^{-1}–$2 \cdot 10^{-2}$s^{-1}	o_b/o_f was determined to be ~5 nM. At the 100 mM Na^+ and in the absence of K^+, an apparent strophanthidin affinity of 100 nM results.

$\alpha = 0.25$: transitions $Na_2 \cdot E_1 \rightarrow Na_3 \cdot E_1$ and $Na_2 \cdot E_1 \cdot ATP \rightarrow Na_3 \cdot E_1 \cdot ATP$

(electrogenic binding/release of 1 Na^+ ion at the cytoplasmic face)

$\beta = 0.75$: transition $(Na_3) \cdot E_1\text{-}P \rightarrow P\text{-}E_2 \cdot (Na_2)$

(electrogenic release/binding of the first Na^+ ion from the neutral binding site)

$\delta_1 = \delta_2 = 0.1$: transitions $P\text{-}E_2 \cdot Na_2 \rightarrow P\text{-}E_2 \cdot Na$ and $P\text{-}E_2 \cdot Na \rightarrow P\text{-}E_2$

(electrogenic release of the two remaining Na^+ ions from the charged binding sites)

$\epsilon_1 = \epsilon_2 = 0.1$: transitions $P\text{-}E_2 \rightarrow P\text{-}E_2 \cdot K$ and $P\text{-}E_2 \cdot K \rightarrow P\text{-}E_2 \cdot K_2$

(electrogenic binding/release of two K^+ ions at the extracellular site)

$\gamma = 1.8$: transition $P\text{-}E_2 \rightarrow E_1$

(spontaneous dephosphorylation without ion transport $P\text{-}E_2 \rightarrow E_1$).

The dielectric coefficients of the transitions between all other states were assumed to be zero. According to the net charge transferred across the entire membrane in each pump cycle, the equations $\alpha + \beta + \delta_1 + \delta_2 + \gamma = 3$ and $\alpha + \beta + \delta_1 + \delta_2 + \epsilon_1 + \epsilon_2 = 1$ hold.

DISCUSSION

In this study we have tried to determine the rate constants of several partial reactions of the Na,K-ATPase. Concentration jump relaxation experiments have been used as a technique by which it is possible to yield information on kinetic and energetic properties of the ion pump which cannot be obtained easily by other methods. For this purpose, we used open membrane fragments with a high density of active proteins obtained from rabbit kidney with two fluorescent labels: 5-IAF to detect conformational changes of the enzyme and RH 421 to analyze electrogenic partial reactions. We also measured transient electric currents, which can be observed after adsorption of membrane fragments to a planar lipid bilayer. The experimental findings have been compared with numerical simulations of a mathematical model of the Na,K-ATPase. All simulations were performed with a single set of parameters without any adjustments.

Cytoplasmic Sodium Binding

As demonstrated clearly in Fig. 5, Na^+ ions bind to the E_1 form of the Na,K-ATPase with an electrogenic component. The detected electrogenic effect is specific for Na^+ ions. No other ions produced a fluorescence decrease. The Na^+-induced fluorescence decrease was independent of the initial protein conformation. Divalent cations like Mg^{2+} did not modify the amplitude of the Na^+-induced fluorescence change, but shifted the affinity of Na^+ binding from 0.8 (0 Mg^{2+}) to 8 mM (10 mM Mg^{2+}). Hill plots of the concentration dependence revealed a Mg^{2+} dependent cooperativity of Na^+ binding. This observation was not Mg^{2+} specific but was also produced by Ca^{2+} or Ba^+ ions. The time course of the Na^+ dependent fluorescence decrease could not be resolved. Indirect evidence that Na^+ binding kinetics are not diffusion limited, has

been obtained by phosphorylation experiments. These studies showed that enzyme phosphorylation is faster upon preincubation of the unphosphorylated enzyme with Na^+ ions (Mårdh and Post, 1977; Hobbs et al., 1988; Froehlich and Fendler, 1991).

These findings do not permit a description of the structure and the process of Na^+ binding, however, they contain some constraints which are observed by the following hypothesis: two of the cytoplasmic ion binding sites may be temporarily occupied by different cations present in the electrolyte. They are identified with the two negatively-charged sites, which are located on the protein surface in the E_1 conformation (Karlish, 1979; Skou and Esmann, 1981; Karlish and Stein, 1985; Mezele, Lewitzki, Ruf, and Grell, 1988; Grell et al., 1991; Arguello and Kaplan, 1991). The effect of divalent cations could be an unspecific competition between Na^+ and these ions at these sites. The third Na^+ ion is assumed to bind to a highly selective Na^+ site within the protein dielectric. Occupying this binding site produces an electrogenic contribution to the ion transport.

Phosphorylation by ATP

The ATP dependence of fluorescence changes associated with the conformational transition $E_1 \rightarrow E_2$ could be studied with 5-IAF and RH 421. From the dependence of the relative fluorescence changes on ATP concentration and their time course (Fig. 6), apparent affinities of 60 nM (5-IAF) and 80 nM (RH 421) ATP were obtained with respect to the amplitudes and 1.2 μM (IAF) and 1.8 μM (RH 421) ATP with respect to the time dependence. These values agree fairly well with equilibrium dissociation values reported in the literature (Nørby and Jensen, 1971; Hegyvary and Post, 1971). Values of $a_f = 1.5 \cdot 10^7\ M^{-1}\ s^{-1}$ and $a_b = 1.6\ s^{-1}$ produced reasonable agreement with all sets of data and correspond to an equilibrium dissociation constant of 0.1 μM.

Enzyme phosphorylation cannot be measured by the fluorescence methods. However, from Na^+ activation of the fluorescence changes associated with the conformational transition $E_1 \rightarrow E_2$, the rate of enzyme phosphorylation could be estimated (Fig. 8). The value $p_f = 200\ s^{-1}$ reproduced the data and is in accordance with data reported in the literature (Mårdh and Zetterquist, 1974; Hobbs et al., 1988; Froehlich and Fendler, 1991). Because all experiments were performed in the nominal absence of ADP, the backward directed rate constant, $p_b = 3.7 \cdot 10^5\ M^{-1}\ s^{-1}$, could not be obtained experimentally. It had to be derived from the principle of microscopic reversibility (see Appendix). This value should be taken only as a rough estimate.

Extracellular Sodium Binding and Release

In K^+-free media the amplitude of fluorescence change, generated by enzyme phosphorylation, is reduced at high Na^+ concentration (Fig. 7). As mentioned above this decrease of $\Delta F/F_o$ is likely to result from a Na^+-induced shift between states $(Na_3) \cdot E_1\text{-}P \leftrightarrow P\text{-}E_2 \cdot (Na_2) \leftrightarrow P\text{-}E_2$ to the left at high Na^+ concentrations (Yoda and Yoda, 1987; Klodos and Nørby, 1988). It is also known from the literature that the distribution between these states depends on membrane potential (Nakao and Gadsby, 1986) and may be affected by adsorption of hydrophobic ions (Stürmer et al., 1991*b*).

To determine equilibrium binding constants of the extracellular Na^+ binding sites,

the following considerations have been taken into account. Upon phosphorylation with ATP in the absence of K^+ ions the enzyme is distributed between states $(Na_3)\cdot E_1\text{-}P \leftrightarrow P\text{-}E_2\cdot(Na_2) \leftrightarrow P\text{-}E_2\cdot(Na) \leftrightarrow P\text{-}E_2$ when it is in a steady state. The population of each state is a function of its affinity for Na^+ and of the Na^+ concentration (which is controlled experimentally). Thus, it is not possible to trigger reactions in which the enzyme performs only a transition between two single states. Therefore, different series of experiments (and controls) had to be performed to assign specific affinities to the three transitions and to determine the rate limiting step. Three different experimental techniques have been used.

Firstly the fluorescent dye RH 421 with its sensitivity to the local electric field has been applied to distinguish differently charged states of the enzyme. In 2 M Na^+ no fluorescence change can be observed upon phosphorylation. Under this condition $(Na_3)\cdot E_1\text{-}P$ is the highest populated state, and the measured fluorescence level has been assigned to this state. In low Na^+ ($\sim$20 mM) steady state is shifted to $P\text{-}E_2$ upon phosphorylation. It is the state with the lowest positive charge density in the protein dielectric and it was used to define the fluorescence level of state $P\text{-}E_2$. A third well defined level is obtained upon inhibition by cardiac steroids. In this state, two Na^+ ions are occluded (Jørgensen and Andersen, 1988; Jørgensen, 1991). This fluorescence level was independent of the (extracellular) Na^+ concentration (Stürmer and Apell, 1992). The second method applied made use of the ability of the 5-IAF label to discriminate between state $(Na_3)\cdot E_1\text{-}P$ and all $P\text{-}E_2$ states (Stürmer et al., 1989). This property has been used to detect the kinetics of the conformational transition $E_1\text{-}P \rightarrow P\text{-}E_2$ in the absence of K^+ and to estimate the relative population of states $(Na_3)\cdot E_1\text{-}P$ and $P\text{-}E_2$. By the third technique charge transport has been observed by measurements of transient electric currents in membrane fragments coupled capacitively to planar lipid bilayers. The transferred charge has been determined in the presence and absence of *CS*. The comparison of the transported charge allowed the assignment of dielectric coefficients (Figs. 14, 15).

In one series of experiments the Na^+ concentration has been varied between 10 mM and 1 M and the RH 421 and 5-IAF fluorescence changes have been recorded (Fig. 7). The decrease of the fluorescence changes with increasing Na^+ concentration is the consequence of a successively higher amount of enzyme with three Na^+ ions bound (RH 421) and of a higher population of the state $(Na_3)\cdot E_1\text{-}P$ (5-IAF). All three binding affinities contribute in these experiments.

Since these experiments can be performed with time-resolved detection of the fluorescence, the relaxation time contains additional information (Fig. 9). At Na^+ concentrations above 10 mM the time course was not significantly concentration dependent and had a rate constant of 20–25 s^{-1} (20°C). This indicated that the rate limiting step was not dependent on the Na^+ concentration and it has been assigned to g_{3f} (see below).

In 2 M NaCl addition of *CS* to the phosphorylated enzyme induced the reaction $(Na_3)\cdot E_1\text{-}P \rightarrow P\text{-}E_2\cdot(Na_2)\cdot CS$. The conformational transition can be detected by 5-IAF-labeled protein (Fig. 11). In the presence of a high *CS* concentration (>100 μM), after complete enzyme inhibition a fluorescence level has been obtained which corresponded quantitatively to that of the $P\text{-}E_2$ states. When, on the other hand, the reaction sequence was started by addition of ATP (*a*) in the presence of CS and 2 M

Na^+ or (*b*) in the presence of 20 mM Na^+ (and high ionic strength) and in the absence of CS, the time course of the 5-IAF signal was not significantly different (data not shown). Independent of the steady states reached after phosphorylation, $P\text{-}E_2\cdot(Na_2)\cdot CS$ or $P\text{-}E_2$, respectively, the level of the 5-IAF fluorescence was the same. This observation is a strong indication that 5-IAF detects the $E_1 \rightarrow E_2$ transition, which is correlated with the release of the first Na^+ (RH 421). Additional evidence has been found in experiments with various concentrations of Na^+ and high concentrations of strophanthidin (> 200 μM). While in the absence of *CS* the 5-IAF fluorescence dropped with increasing Na^+ concentrations, the fluorescence level after phosphorylation remained constant in the presence of *CS*, independent of the actual Na^+ concentration. It was equal to the level at low Na^+. This is a confirmation of the explanation that 5-IAF detects the conformational transition $(Na_3)\cdot E_1\text{-}P \leftrightarrow P\text{-}E_2\cdot(Na_2)$, but is not affected by the release of the subsequent two Na^+ ions, $P\text{-}E_2\cdot(Na_2) \rightarrow P\text{-}E_2\cdot(Na) \rightarrow P\text{-}E_2$.

When the phosphorylation reaction is started in buffers containing 100 mM Na^+ and different concentrations of strophanthidin, biphasic RH 421 fluorescence signals can be observed in the presence of intermediate inhibitor concentrations (Fig. 10). The concentration dependence of these fluorescence signals can be explained in the following way. The release of Na^+ to the extracellular side involves two distinct electrogenic steps, $(Na_3)\cdot E_1\text{-}P \leftrightarrow P\text{-}E_2\cdot(Na_2)$ and $P\text{-}E_2\cdot(Na_2) \leftrightarrow P\text{-}E_2$. The first electrogenic step consists in the release of 1 Na^+ ion from the neutral binding site to the extracellular face and is correlated with the conformational transition $E_1 \leftrightarrow E_2$. The second electrogenic step accounts for the release of the remaining 2 Na^+ ions from their negatively charged binding sites through a narrow access channel (Stürmer and Apell, 1992). In the absence of CS the pump proceeds through the whole reaction sequence to state $P\text{-}E_2$ when started by enzyme phosphorylation. However, in the presence of high CS the pump is almost immediately trapped in state $P\text{-}E_2\cdot(Na_2)\cdot CS$, which has a lower fluorescence intensity than $P\text{-}E_2$. In a concentration range of 10 and 40 μM strophanthidin the reaction is branched significantly in state $P\text{-}E_2(Na_2)$, because the reaction rates of both pathways become comparable. As a consequence the fluorescence is transiently increased as shown in Fig. 10. The kinetic analysis allowed an estimation of g_{2f} and g_{1f} as given in Table V. A lower limit of these rate constants can be estimated from competition experiments with K^+ ions (see next section of the discussion).

The dielectric coefficients of this electrogenic reaction sequence could be determined by measurements of transient electrical pump currents. At low Na^+ concentrations (50–200 mM) the charge transferred upon phosphorylation is not significantly different in the presence and absence of strophanthidin (Fig. 12 *A*). Since it has been proven that the enzyme can be inhibited completely by strophanthidin, it must be concluded that the charge, which is transferred in the reaction $(Na_3)\cdot E_1\text{-}P \leftrightarrow P\text{-}E_2\cdot(Na_2)$, is not significantly smaller than the charge transferred in the absence of the inhibitor, when the enzyme runs through the whole sequence of steps $(Na_3)\cdot E_1\text{-}P \rightarrow \ldots \rightarrow P\text{-}E_2$. The preceding phosphorylation step $Na_3\cdot E_1\cdot ATP \rightarrow (Na_3)\cdot E_1\text{-}P$ can be neglected, because it has been shown to be electroneutral (Borlinghaus et al., 1987). At Na^+ concentrations above 500 mM the ratio *S* of transferred charge in the absence and presence of *CS* was decreased (Fig. 13). While the transferred charge in

the presence of the inhibitor remained essentially unchanged in the whole concentration range, the charge before addition of *CS* became smaller with increasing Na^+. This discrepancy is also reflected in the current signals of Fig. 12. In 2.2 M NaCl, where 93% of the enzyme is in state $(Na_3)\cdot E_1$-*P* after phosphorylation in the absence of *CS*, the ratio *S* became smaller than 0.19, which indicates a significant *CS*-induced charge movement.

These findings produce a strong constraint for the involved rate constants (g_{3f}, g_{2f}, g_{1f}, g_{3b}, g_{2b}, g_{1b}) and their dielectric coefficients. Analysis of the experiments by numerical simulations, which reproduced the experiments concerning the conformational change and the release and binding of extracellular Na^+ ions, are compiled in Table V. It is noteworthy that we could not find a different set of rate constants outside the range of confidence which would describe all the presented experiments. The equilibrium dissociation constants found by simulation are 120 mM (g_{3f}/g_{3b}), 1.8 M (g_{2f}/g_{2b}) and 100 mM (g_{1f}/g_{1b}). The fractions of phosphorylated enzyme in the different states are listed as function of the Na^+ concentration in Table I.

In the literature the determination of the extracellular affinity for Na^+ is scanty due to the difficulties of appropriate experimental techniques. Apparent affinities of the overall Na^+ binding on the extracellular side have been published to be 0.5 mM for inhibition of the Na^+ efflux (Glynn and Karlish, 1976), <5 mM for ATP:ADP exchange (Kaplan and Hollis, 1980; Kaplan, 1982), 31 mM for stimulation of Na^+–Na^+ exchange (Garay and Garrahan, 1973) and 600 mM for ATP synthesis (Taniguchi and Post, 1975). A theoretical approach to get information on extracellular binding affinities has been undertaken by Pedemonte (1988). He proposed dissociation constants of 1 M, 50 and 0.5 mM from computer simulations of a modified Post-Albers scheme to account qualitatively for the high-affinity Na^+ inhibition of the Na-ATPase and the ATP/ADP exchange activities. However, the effect of high-affinity Na^+ inhibition of red blood cells, which was described by Pedemonte's set of numbers, could be reproduced also in the framework of our model with our set of parameters in Table V, as shown in the inset of Fig. 19.

The rate limiting step has been identified to be $(Na_3)\cdot E_1\text{-}P \rightarrow P\text{-}E_2\cdot(Na_2)$. Conformational transition and release of the first Na^+ ion could not be discriminated with the experimental techniques applied in this paper. Therefore both reactions are treated as one step. The corresponding rate has been determined to be $g_{3f} = 22\ s^{-1}$ (T = 20°C). From voltage-jump current-relaxation studies performed in the presence of Na^+ ions and ATP and in the absence of K^+ ions, rate constants of 200 s^{-1} (36°C) have been obtained for Na^+ binding and release in cardiac myocytes (Nakao and Gadsby, 1986). With an activation energy of 90–110 kJ/mol a rate constant of 20–25 s^{-1} is calculated at 20°C. The similarity between this rate limiting constant in electric relaxation studies and in the conformational transition $E_1\text{-}P \rightarrow P\text{-}E_2$ can be taken as further support of the presented model, in which the step $(Na_3)\cdot E_1\text{-}P \leftrightarrow P\text{-}E_2\cdot(Na_2)$ is the rate limiting and essential voltage-dependent partial reaction of the Na^+ translocation.

This is also reflected in the dielectric coefficients which can be determined in detail by the experimental constraint of the data in Fig. 13. The fit to the data in Fig. 13 led to $S = 1.27$ for Na^+ concentrations close to zero, where state $(Na_3)\cdot E_1\text{-}P$ is no longer populated (not shown). According to Eq. 10 the ratio of $(\delta_1 + \delta_2)/\beta$ is 0.27. Together

with the rest of the presented data a consistent description is given by $\beta = 0.75$ (i.e., reaction $(Na_3)\cdot E_1\text{-}P \leftrightarrow P\text{-}E_2\cdot(Na_2)$ carries one elementary charge across 75% of the membrane dielectric) and $\delta_1 + \delta_2 = 0.2$ (in the subsequent reaction $P\text{-}E_2\cdot(Na_2) \leftrightarrow P\text{-}E_2\cdot(Na(Na) \leftrightarrow P\text{-}E_2$ one elementary charge is moved across 20% of the membrane dielectric). Since two ions are released/bound we have assigned $\delta_1 = \delta_2 = 0.1$ due to lack of more detailed experimental information. The dielectric coefficient of the electrogenic binding of Na^+ on the cytoplasmic side is set to $\alpha = 0.25$, which fulfills the constraint that one ion transverses the membrane electronically: $\alpha + \beta = 1$.

External Potassium Binding

Potassium binding was studied in fluorescence experiments, in which ATP was released in a buffer containing high concentrations of Na^+ and millimolar concentrations of K^+. In these experiments 5-IAF and RH 421-labeled enzyme showed biphasic fluorescence traces in the presence of K^+ (Fig. 14, *A* and *B*). Amplitudes and time course of these fluorescence curves have been used to estimate rate constants of K^+ binding and apparent K^+ affinities. The apparent K^+ affinity and the kinetics of K^+ binding depended on Na^+ and ATP concentration (Tables II and III). The dependence on Na^+ can be explained by the assumption that Na^+ and K^+ compete for the same binding sites. Similar results have been obtained also by other methods. Labeling studies with DCCD and DEAC gave evidence for the involvement of two carboxyl groups in ion binding (Shani-Sekler, Goldshleger, Tal, and Karlish, 1988; Karlish, Goldshleger, and Stein, 1990; Karlish, Goldshleger, Tal, and Stein, 1991; Arguello and Kaplan, 1991). It was suggested, that two K^+ or two Na^+ ions combine with these carboxyls. Rapid dephosphorylation studies showed also that K^+-induced dephosphorylation is less effective in high Na^+ concentrations (Klodos and Forbush, 1991). The dependence of the apparent K^+ affinity on ATP concentration can be explained in the following way. At very low ATP concentrations, the conformational transition occurs via $E_2(K_2) \leftrightarrow K_2\cdot E_1$ with a rate, h_f, of less than 0.5 s^{-1}. This is slower than the rate of K^+ binding even at low K^+ concentrations. Therefore the apparent K^+ affinity will approach the intrinsic binding affinity at very low ATP concentrations. It has been estimated to be ~35 μM from experiments with enzyme phosphorylated by phosphate or acetyl phosphate (unpublished results). At high ATP concentrations, the transition $E_2(K_2) \rightarrow E_2(K_2)\cdot ATP \rightarrow K_2E_1$ is activated and the turnover rate is much higher. Thus, the apparent K^+ affinity is lower.

A lower limit of the rate of Na^+ release from state $P\text{-}E_2(Na_2)$ can be estimated from competition experiments presented in Figs. 16 and 17. In these experiments, RH 421-labeled membrane fragments were incubated in 200 mM Na^+ and various concentrations of K^+ and strophanthidin. Because strophanthidin binds only to state $P\text{-}E_2(Na_2)$ and slightly to $P\text{-}E_2(K_2)$, the strophanthidin binding kinetics and its apparent affinity depend on the portion of enzyme present in these states. Assuming a fast release of sodium from state $P\text{-}E_2(Na_2)$ and a fast enzyme dephosphorylation, the portion of the enzyme in state $P\text{-}E_2(Na_2)$ must be expected to depend on K^+ concentration, which promotes the forward reaction. We found that strophanthidin is bound much faster in the presence of 4 mM KCl than 20 mM KCl (Fig. 15). Numerical simulations, which reproduced the experimental findings, require that the rates of Na^+ release, g_{2f} and g_{1f}, must be higher than 2,000 s^{-1}. Independent

experiments, in which the apparent binding affinity of anthroylouabain is investigated as function of K^+ concentration, and their numerical simulation (Table IV) support the conclusion that the population of state $P\text{-}E_2(Na_2)$ is dependent on K^+.

Further information on the rate of Na^+ release from state $P\text{-}E_2(Na_2)$ comes from experiments in which inhibition of the enzymatic activity by strophanthidin has been studied in the presence of various K^+ concentrations. In these experiments the inhibition kinetics and the apparent strophanthidin affinity depended strongly on the K^+ concentration (Fig. 16). This effect of K^+ saturated for high concentrations. It can be explained assuming that Na^+ release becomes rate limiting in the reaction sequence $P\text{-}E_2\cdot(Na_2) \leftrightarrow P\text{-}E_2\cdot(Na) \leftrightarrow P\text{-}E_2 \leftrightarrow P\text{-}E_2\cdot(K) \leftrightarrow P\text{-}E_2\cdot(K_2) \leftrightarrow E_2(K_2)$ when $[K^+] > 40$ mM. An alternative reason could be that the rate of K^+ binding saturates in concentrations above 40 mM. A third explanation would be the assumption of a rate-limiting enzyme dephosphorylation. A discrimination is not possible so far. However, from numerical simulations of the reaction cycle, a lower limit of 5,000 s^{-1} can be estimated for extracellular Na^+ release. The proposed model of *CS* binding does not only give a quantitative description of the well known potassium-ouabain antagonism, but also explains the apparent paradox that K^+ may prevent ouabain binding although the enzyme is able to occlude K^+ ions by CS binding (Forbush, 1983; Jørgensen, 1991). The observation, that pretreatment of the enzyme with ouabain prevents K^+ occlusion (Glynn and Richards, 1982) can be explained by the assumption, that the access to the ion binding sites from the extracellular side is blocked by ouabain.

Conformational Transitions E_2 to E_1

The conformational transition $E_2 \rightarrow E_1$ was studied using 5-IAF-labeled membrane fragments. From the ATP dependence of the time course and of the amplitudes of the 5-IAF fluorescence change, apparent ATP affinities were obtained with respect to the time course (8 μM) and to the amplitudes (2 μM) as derived from Fig. 17. These values are smaller than the values reported in the literature but indicate clearly that ATP promotes the conformational change $E_2 \rightarrow E_1$ by acting on the low affinity ATP binding site. From optical experiments using intrinsic tryptophan fluorescence, a value of 450 μM has been estimated (Karlish and Yates, 1978). From studies of ATP-induced ^{86}Rb deocclusion, Forbush (1987*a*) obtained a value of 290 μM. Measurements of K–K exchange resulted in an apparent affinity of 110 μM (Sachs, 1981). Under turnover conditions in reconstituted vesicles with the same enzyme 13 μM have been obtained (Apell et al., 1990). The K^+ dependence of the ATP-induced fluorescence change can be explained in the following way: in the presence of millimolar concentrations of K^+ and in the absence of Na^+ and nucleotides, a substantial fraction of the enzyme is initially present in state $E_2(K_2)$. Low-affinity binding of ATP shifts the equilibrium back to state E_1, which increases the 5-IAF fluorescence. However, in the presence of higher K^+ concentrations a reasonable amount of K^+ remains bound to state $ATP\cdot E_2(K_2)$. This effect produced the observed smaller 5-IAF fluorescence increase at higher K^+ concentrations.

The enzymatic activity of Na,K-ATPase prepared from rabbit kidney was measured as a function of Na^+ and K^+ concentrations (Fig. 19). Performing a numerical simulation of these experiments, we found that the set of kinetic parameters, which

was obtained from the simulation of the presented optical and electric experiments, described consistently the Na^+ and K^+ dependence of enzymatic activity (Fig. 19). This verification of the model and the applied set of parameters by a completely different set of experiments is a strong support for the presented approach. The difference of our experimental data, obtained with enzyme from rabbit kidney compared to previously published data of enzyme prepared from ox brain (Skou, 1975), reflects a distinction of kinetic rather than mechanistic properties. These obviously species-specific differences of binding affinities or rate constants point out that kinetic parameters obtained from different tissues may be compared only with restrictions. The values given for the kinetic parameters (Table V) of the pump cycle (Fig. 3) should be taken only as an estimate for enzyme from other sources.

The Electrostatic Model of the Na,K-ATPase

Numerical simulations have been performed on the basis of the modified Post-Albers scheme (Fig. 3) with the set of parameters presented in Table V. It has been stated

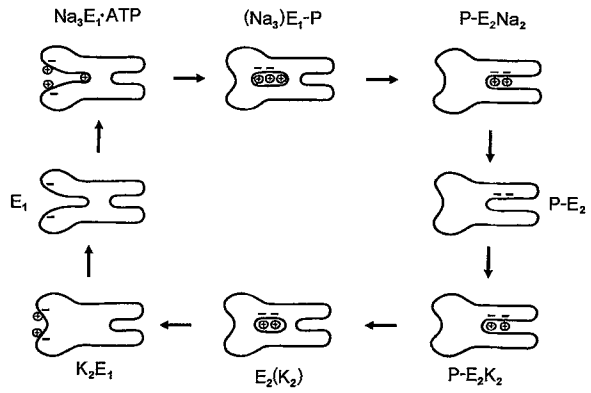

FIGURE 20. An electrostatic model of the Na,K-pump. For details see text.

already that all lines drawn in the figures, which are indicated as simulation, are not fits but straight-forward calculations with the same set of parameters. The good agreement between data and simulation justifies the presentation of an electrostatic model of ion transport under physiological conditions as shown in Fig. 20, which includes all features implemented in the mathematical model.

In the nonoccluded E_1 states of the enzyme two negatively charged binding sites are accessible in the (electrostatic) surface of the pump. K^+ ions and (with higher affinity) two Na^+ ions compete for the same sites, which probably contain negatively charged carboxyl residues. The third binding site is neutral and highly specific for Na^+. Ion binding to this site is electrogenic. This property is a strong indication of a location inside of the protein dielectric.

Na^+ occlusion by enzyme phosphorylation with ATP occurs when all three binding sites are occupied and is not accompanied by an electrogenic effect. Therefore, the Na^+ ion bound at the neutral binding site is not moved within the protein dielectric during the transition $Na_3 \cdot E_1 \cdot ATP \rightarrow (Na_3) \cdot E_1\text{-}P$. The occlusion thus consists probably

only in the closure of a gate. The conformational transition into state E_2 is correlated with an access of the binding sites to the extracellular phase and the release of the first Na^+ ion from the neutral binding site. This step represents the major electrogenic contribution of the whole cycle.

Since the release of the successive two Na^+ ions has been shown to be electrogenic and consequently also the binding of the two K^+ ions to the same (negatively charged) binding sites, it can be concluded that these sites are located within the protein dielectric of the protein in the states of P-E_2. Therefore the connection between sites and aqueous phase is thought to be formed by a narrow access channel ("ion well"). Cardiac steroids inhibit the enzyme by blocking P-E_2 states in which two cations, Na^+ or K^+, are bound.

Binding of K^+ ions in the E_2 conformation occurs also by an electrogenic process through the proposed access channel. Occlusion of two K^+ ions, dephosphorylation, conformational change $E_2 \rightarrow E_1$ and release of K^+ into the cytoplasmic phase are electroneutral processes, because the cations are paired by negatively charged binding sites which have direct access to the aqueous phase in conformation E_1.

APPENDIX

Numerical Simulation of the Reaction Scheme Shown in Fig. 3

We denote the fraction of pump molecules in state A by $x[A]$ and introduce the following variables:

$$x_1 \equiv x[Na_2 \cdot E_1] + x[Na \cdot E_1] + x[E_1] + x[K \cdot E_1] + x[K_2 \cdot E_1]$$

$$x_2 \equiv x[Na_3 \cdot E_1]$$

$$x_3 \equiv x[Na_2 \cdot E_1 \cdot ATP] + x[Na \cdot E_1 \cdot ATP] + x[E_1 \cdot ATP] + x[K \cdot E_1 \cdot ATP] + x[K_2 \cdot E_1 \cdot ATP]$$

$$x_4 \equiv x[Na_3 \cdot E_1 \cdot ATP]$$

$$x_5 \equiv x[(Na_3) \cdot E_1\text{-}P]$$

$$x_6 \equiv x[P\text{-}E_2 \cdot (Na_2)]$$

$$x_7 \equiv x[P\text{-}E_2 \cdot (Na)]$$

$$x_8 \equiv x[P\text{-}E_2]$$

$$x_9 \equiv x[P\text{-}E_2 \cdot (K)]$$

$$x_{10} \equiv x[P\text{-}E_2 \cdot (K_2)]$$

$$x_{11} \equiv x[E_2 \cdot (K_2)]$$

$$x_{12} \equiv x[ATP \cdot E_2 \cdot (K_2)]$$

$$x_{13} \equiv x[E_2 \cdot (Na_2)]$$

$$x_{14} \equiv x[P\text{-}E_2 \cdot (Na_2) \cdot CS]$$

$$x_{15} \equiv x[P\text{-}E_2 \cdot (K_2) \cdot CS].$$

According to the scheme in Fig. 3, the time derivatives of x_i are given by

$$\dot{x}_1 = -\left[a_f \cdot c_T + r_b \cdot c_P \cdot \frac{1}{P'} + h_b \cdot \frac{k_1^{(1)} \cdot k_2^{(1)}}{P'} + e_b \cdot \frac{n_1^{(1)} \cdot n_2^{(1)}}{P'} + n_{3f} \cdot c_{Na}^1 \cdot \frac{n_1^{(1)} \cdot n_2^{(1)}}{P'}\right] x_1 + n_{3b} \cdot x_2 + a_b \cdot x_3 + r_f \cdot x_8 + h_f \cdot x_{11} + e_f \cdot x_{13}$$

$$\dot{x}_2 = -[n_{3b} + a_f \cdot c_T] \cdot x_2 + n_{3f} \cdot c'_{Na} \cdot \frac{n_1^{(1)} \cdot n_2^{(1)}}{P'} x_1 + a_b \cdot x_4$$

$$\dot{x}_3 = -\left[a_b + c_{Na}^1 \cdot n_3^f \cdot \frac{n_1^{(1)} \cdot n_2^{(1)}}{P'} + k_b \cdot \frac{k_1^{(1)} \cdot k_2^{(1)}}{P'}\right] x_3 + a_f \cdot c_T \cdot x_1 + n_{3b} \cdot x_4 + k_f \cdot x_{12}$$

$$\dot{x}_4 = -[p_f + a_b + n_{3b}] x_4 + a_f \cdot c_T \cdot x_2 + c_{N'} \cdot n_{3f} \cdot \frac{n_1^{(1)} \cdot n_2^{(1)}}{P'} \cdot x_3 + p_b \cdot c_D \cdot x_5$$

$$\dot{x}_5 = -[p_b \cdot c_D + g_{3f}] x_5 + p_f \cdot x_4 + g_{3b} \cdot c_N^{(2)} \cdot x_6$$

$$\dot{x}_6 = -[g_{3b} \cdot c_{Na}^{(2)} + g_{2f} + d_f + o_f \cdot c_{ou}] \cdot x_6 + g_{3f} \cdot x_5 + d_b \cdot c_p \cdot x_{13} + g_{2b} \cdot c_{Na}^{(2)} \cdot x_7 + o_b \cdot x_{14}$$

$$\dot{x}_7 = -[g_{2b} \cdot c_{Na}^{(2)} + g_{1f}] \cdot x_7 + g_{2f} \cdot x_6 + g_{1b} \cdot c_{Na}^{(2)} \cdot x_8$$

$$\dot{x}_8 = -[g_{1b} \cdot c_{Na}^{(2)} + m_{1f} \cdot c_K^{(2)} + r_f] \cdot x_8 + g_{1f} \cdot x_7 + m_{1b} \cdot x_9 + \frac{1}{P'} \cdot x_1 \cdot r_b \cdot c_p$$

$$\dot{x}_9 = -[m_{1b} + m_{2f} \cdot c_K^{(2)}] \cdot x_9 + m_{1f} \cdot c_K^{(2)} \cdot x_8 + m_{2b} \cdot x_{10}$$

$$\dot{x}_{10} = -[m_{2b} + q_f] \cdot x_{10} + q_b \cdot c_p \cdot x_{11} + m_{2f} \cdot c_K^{(2)} \cdot x_9 + o_b \cdot x_{15}$$

$$\dot{x}_{11} = -[q_b \cdot c_p + s_f \cdot c_T + h_g] \cdot x_{11} + q_f \cdot x_{10} + s_b \cdot x_{12} + h_b \cdot \frac{k_K^{(1)} \cdot k_K^{(2)}}{P'} \cdot x_1$$

$$\dot{x}_{12} = -[k_f + s_b] \cdot x_{12} + s_f \cdot c_T \cdot x_{11} + k_b \cdot \frac{k_1^{(1)} \cdot k_2^{(1)}}{P'} x_3$$

$$\dot{x}_{13} = -[d_b \cdot c_p + e_f] \cdot x_{13} + e_b \cdot \frac{n_1^{(1)} \cdot n_2^{(1)}}{P'} \cdot x_1 + d_f \cdot x_6$$

$$\dot{x}_{14} = -o_b \cdot x_{14} + o_f \cdot c_{ou} \cdot x_6$$

$$\dot{x}_{15} = -o_b \cdot x_{15} + o_f \cdot c_{ou} \cdot x_{10}.$$

In the equations given above, the following relations have been used:

$$x[Na_2 \cdot E_1] = x_1 \cdot \frac{n_1^1 \cdot n_2^1}{P'}$$

$$x[Na_2 \cdot E_1 \cdot ATP] = x_3 \cdot \frac{n_1^1 \cdot n_2^1}{P'}$$

$$x[K_2 \cdot E_1] = x_1 \cdot \frac{k_1^1 \cdot k_2^1}{P'}$$

$$x[K_2 \cdot E_1 \cdot \mathrm{ATP}] = x_3 \cdot \frac{k_1^1 \cdot k_2^1}{P'}$$

$$n_i^1 = \frac{c_{\mathrm{Na,i}}^1}{K_{\mathrm{Na,i}}^1} = \frac{x[\mathrm{Na}_i \cdot E_1]}{x[\mathrm{Na}_{i-1} \cdot E_1]} = \frac{x[\mathrm{Na}_i \cdot E_1 \cdot \mathrm{ATP}]}{x[\mathrm{Na}_{i-1} \cdot E_1 \cdot \mathrm{ATP}]}; \qquad i = 1, 2$$

$$k_i^1 = \frac{c_{\mathrm{Ki}}^1}{K_{\mathrm{Ki}}^1} = \frac{x[K_i \cdot E_1]}{x[K_{i-1} \cdot E_1]} = \frac{x[K_i \cdot E_1 \cdot \mathrm{ATP}]}{x[K_{i-1} \cdot E_1 \cdot \mathrm{ATP}]}; \qquad i = 1, 2$$

$$P' = 1 + n_1^1 + n_2^1 + k_1^1 + k_1^1 \cdot k_2^1.$$

Four rate (or equilibrium) constants of the reaction scheme in Fig. 3 are determined by the principle of detailed balance:

$$p_b = \frac{K_{K1} \cdot K_{K2}}{K_{Na1} \cdot K_{Na2}} \cdot \frac{\bar{c}_T}{\bar{c}_D \cdot \bar{c}_P} \cdot \frac{n_{3f} \cdot k_f \cdot g_{3f} \cdot g_{2f} \cdot g_{1f} \cdot m_{1f} \cdot m_{2f} \cdot q_f \cdot s_f \cdot p_f}{n_{3b} \cdot k_b \cdot g_{3b} \cdot g_{2b} \cdot g_{1b} \cdot m_{1b} \cdot m_{2b} \cdot q_b \cdot s_b}$$

$$a_b = \frac{a_f \cdot k_b \cdot s_b \cdot h_f}{k_f \cdot s_f \cdot h_b}$$

$$r_b = \frac{1}{K_{Na1} \cdot K_{K1}} \cdot \left(\frac{c_k^1}{c_k^2}\right) \cdot \frac{\alpha_f \cdot k_b \cdot s_b \cdot q_b \cdot m_{2b} \cdot m_{1b} \cdot r_f}{a_b \cdot k_f \cdot s_f \cdot q_f \cdot m_{2f} \cdot m_{1f}}$$

$$d_b = \frac{\bar{c}_T}{\bar{c}_D \cdot \bar{c}_P} \cdot \frac{\alpha_f \cdot p_f \cdot g_{3f} \cdot e_f \cdot n_{3f} \cdot d_f}{a_b \cdot p_b \cdot g_{3b} \cdot e_b \cdot n_{3b}}.$$

The coupled differential equations have been integrated numerically using a Runge-Kutta algorithm. To simulate specific ionic conditions, substrate concentrations and the assignments for rate and equilibrium constants (Table V), for the fluorescence signals, $\Delta F/F_o$, and for the pump currents $I_p(t)$, have been applied. The simulated time courses of fluorescence signals and electric currents are presented as lines in the corresponding figures.

The authors thank G. Witz and M. Roudna for excellent technical assistance, and Dr. S. J. D. Karlish for interesting discussions.

This work has been financially supported by the Deutsche Forschungsgemeinschaft (SFB 156).

Original version received 20 January 1993 and accepted version received 27 April 1994.

REFERENCES

Apell, H.-J., R. Borlinghaus, and P. Läuger. 1987. Fast charge translocation associated with partial reactions of the Na,K-Pump: II. Microscopic analysis of transient currents. *Journal of Membrane Biology.* 97:179–191.

Apell, H.-J., V. Häring, and M. Roudna. 1990. Na,K-ATPase in artificial lipid vesicles: comparison of Na,K and Na-only pumping mode. *Biochimica et Biophysica Acta.* 1023:81–90.

Arguello, J. M., and J. H. Kaplan. 1991. Evidence for essential carboxyls in the cation-binding domain of the Na,K-ATPase. *Journal of Biological Chemistry.* 266:14627–14635.

Askari, A., S. S. Kakar, and W.-H. Huang. 1988. Ligand binding of the ouabain-complexed ($Na^+ + K^+$)-ATPase. *Journal of Biological Chemistry.* 263:235–242.

Bahinski, A., M. Nakao, and D. C. Gadsby. 1988. Potassium translocation by the Na^+,K^+-pump is voltage insensitive. *Proceedings of National Academy of Sciences, USA.* 85:3212–3416.

Baker, P. F., and J. S. Willis. 1970. Potassium ions and the binding of cardiac glycosides to mammalian cells. *Nature.* 226:251–523.

Borlinghaus, R., H.-J. Apell, and P. Läuger. 1987. Fast charge translocation associated with partial reactions of the Na,K-pump: I. Current and voltage transients after photochemical release of ATP. *Journal of Membrane Biology.* 97:161–178.

Bühler, R. 1992. Reaktionskinetische Untersuchungen an der Na,K-ATPase. Hartung-Gorre Verlag, Konstanz. Konstanzer Dissertation Vol. 365.

Bühler, R., W. Stürmer, H.-J. Apell, and P. Läuger. 1991. Charge translocation by the Na,K-pump: I. Kinetics of local field changes studied by time-resolved fluorescence measurements. *Journal of Membrane Biology.* 121:141–161.

Clarke, R. J., P. Schrimpf, and M. Schöneich. 1992. Spectroscopic investigations of the potential-sensitive membrane probe RH 421. *Biochimica et Biophysica Acta.* 1112:142–152.

David, P., and S. J. D. Karlish. 1990. Characterization of lanthanides as competitors of Na^+ and K^+ in occlusion sites of renal (Na^+,K^+)-ATPase. *In* The Sodium Pump. Recent Developments. J. H. Kaplan and P. De Weer, editors. Rockefeller University Press, New York. 427–431.

DeLuca, M., and W. D. McElroy. 1978. Purification and properties of firefly luciferase. *Methods in Enzymology.* 57:3–15.

Erdmann, E., and W. Schoner. 1973. Ouabain-receptor interactions in (Na^+ + K^+)-ATPase preparations from different tissues and species. Determination of kinetic constants and dissociation constants. *Biochimica et Biophysica Acta.* 307:386–398.

Fendler, K., E. Grell, M. Haubs, and E. Bamberg. 1985. Pump currents generated by the purified Na^+,K^+-ATPase from kidney on black lipid membranes. *EMBO Journal.* 4:3079–3085.

Forbush III, B. 1983. Cardiotonic steroid binding to Na,K-ATPase. *In* Current Topics in Membranes and Transport. Vol. 19. J. F. Hoffmann and B. Forbush III, Guest Editors. Academic Press, NY. 167–201.

Forbush III, B. 1984. Na^+ movement in a single turnover of the Na pump. *Proceedings of National Academy of Sciences, USA.* 81:5310–5314.

Forbush III, B. 1987*a*. Rapid release of ^{42}K and ^{86}Rb from an occluded state of the Na,K-pump in the presence of ATP or ADP. *Journal of Biological Chemistry.* 262:11104–11115.

Forbush III, B. 1987*b*. Rapid release of ^{42}K and ^{86}Rb from two distinct transport sites on the Na,K-pump in the presence of P_i or vanadate. *Journal of Biological Chemistry.* 262:11116–11127.

Forbush III, B. 1988. Rapid ^{86}Rb release from an occluded state of the Na,K-pump reflects the rate of dephosphorylation or dearsenylation. *Journal of Biological Chemistry.* **263:**7961–7969.

Forbush III, B., and I. Klodos. 1991. Rate-limiting steps in Na translocation by the Na/K Pump. *In* The Sodium Pump: Structure, Mechanism and Regulation. J. H. Kaplan and P. De Weer, editors. The Rockefeller University Press, New York. 201–209.

Fortes, P. A. G. 1986. A fluorometric method for the determination of functional (Na,K)-ATPase and cardiac glycoside receptors. *Analytical Biochemistry.* 158:454–462.

Fringeli, U. P., H.-J. Apell, M. Fringeli, and P. Läuger. 1989. Polarized infrared absorption of Na^+/K^+-ATPase studied by attenuated total reflection spectroscopy. *Biochimica et Biophysica Acta.* 984:301–312.

Froehlich, J. P., R. W. Albers, G. J. Koval, R. Goebel, and M. Berman. 1976. Evidence for a new intermediate state in the Mechanism of (Na^+ + K^+)-adenosine triphosphatase. *Journal of Biological Chemistry.* 251:2186–2188.

Froehlich, J. P., and K. Fendler. 1991. The partial reactions of the Na^+- and Na^+ + K^+-activated adenosine triphosphatases. *In* The Sodium Pump: Structure, Mechanism and Regulation. J. H. Kaplan and P. De Weer, editors. The Rockefeller University Press, New York. 227–247.

Garray, R. P., and P. J. Garrahan. 1973. The interaction of sodium and potassium with the sodium pump in red cells. *Journal of Physiology.* 231:297–325.

Gadsby, D. C., R. F. Rakowski, and P. De Weer. 1993. Extracellular access to the Na,K-pump: pathway similar to ion channel. *Science.* 260:100–103.

Glynn, I. M. 1985. The Na^+,K^+-transporting adenosine triphosphatase. *In* The Enzymes of Biological Membranes. Vol. 3. A. N. Martonosi, editor. Plenum Publishing Corp., New York. 35–114.

Glynn, I. M., Y. Hara, D. E. Richards, and M. Steinberg. 1987. Comparison of rates of cation release and of conformational change in dog kidney Na,K-ATPase. *Journal of Physiology.* 383:477–485.

Glynn, I. M., and S. J. D. Karlish. 1976. ATP hydrolysis associated with an uncoupled sodium flux through the sodium pump: evidence for allosteric effects of intracellular ATP and extracellular sodium. *Journal of Physiology.* 256:465–496.

Glynn, I. M., and D. E. Richards. 1982. Occlusion of rubidium ions by the sodium-potassium pump: its implications for the mechanism of potassium transport. *Journal of Physiology.* 387:331–355.

Grell, E., R. Warmuth, E. Lewitzki, and H. Ruf. 1991. Precision titrations to determine affinity of alkali, alkaline earth, and buffer binding to Na,K-ATPase. *In* The Sodium Pump. Recent Developments. J. H. Kaplan and P. De Weer, editors. Rockefeller University Press, New York. 441–445.

Grinvald, A., R. Hildesheimer, I. C. Farber, and L. Anglister. 1982. Improved fluorescent probes for the measurements of rapid changes in membrane potential. *Biophysical Journal.* 39:301–308.

Hegyvary, C., and R. L. Post. 1971. Binding of adenosine triphosphate to sodium and potassium ion-stimulated adenosine triphosphatase. *Journal of Biological Chemistry.* 246:5234–5240.

Hobbs, A. S., R. W. Albers, and J. P. Froehlich. 1988. Complex time dependence of phosphoenzyme formation and decomposition in electroplax Na,K-ATPase. *In* The Na^+,K^+-Pump, Part A: Molecular Aspects. Progress in Clinical Biology. Vol. 268A. J. C. Skou, J. G. Nørby, A. B. Maunsbach, and M. Esmann editors. Alan R. Liss, Inc., New York. 307–314.

Jørgensen, P. L. 1974. Isolation of the (Na^+ + K^+)-ATPase. *Methods in Enzymology.* 32:277–290.

Jørgensen, P. L. 1991. Conformational transitions in the α-subunit and ion occlusion. *In* The Sodium Pump: Structure, Mechanism and Regulation. J. H. Kaplan and P. De Weer, editors. Rockefeller University Press, New York. 189–200.

Jørgensen, P. L., and J. P. Andersen. 1988. Structural basis for E_1-E_2 conformational transitions in Na,K-pump and Ca-pump proteins. *Journal of Membrane Biology.* 103:95–120.

Kapakos, J. G., and M. Steinberg. 1982. Fluorescence labeling of (Na,K)-ATPase by 5-iodoacetamidofluorescein. *Biochimica et Biophysica Acta.* 693:493–496.

Kapakos, J. G., and M. Steinberg. 1986. 5-Iodoacetamidofluorescein-labeled (Na,K)-ATPase, Steady-state fluorescence during turnover. *Journal of Biological Chemistry.* 261:2090–2096.

Kaplan, J. H. 1982. Sodium-pump mediated ATP : ADP exchange. *Journal of General Physiology.* 80:915–937.

Kaplan, J. H., and P. J. Hollis. 1980. External Na dependence of ouabain-sensitive ATP:ADP exchange initiated by photolysis of intracellular caged-ATP in human red cell ghosts. *Nature.* 288:587–589.

Karlish, S. J. D. 1979. Cation induced conformational states of Na,K-ATPase studied with fluorescence probes. *In* Na,K-ATPase. Structure and Kinetics. J. C. Skou and J. G. Nørby, editors. Academic Press, New York. 115–128.

Karlish, S. J. D. 1980. Characterization of conformational changes in (Na,K)ATPase labeled with fluorescein at the active site. *Journal of Bioenergetics and Biomembranes.* 12:111–135.

Karlish, S. J. D., R. Goldshleger, and W. D. Stein. 1990. A 19 kDa C-terminal tryptic fragment of the α chain of Na/K-ATPase is essential for occlusion and transport of cations. *Proceedings of the National Academy of Sciences, USA.* 87:4566–4570.

Karlish, S. J. D., R. Goldshleger, P. M. Tal, and W. D. Stein. 1991. Structure of the cation binding sites of Na,K-ATPase. *In* The Sodium Pump: Recent Developments. J. H. Kaplan and P. De Weer, editors. The Rockefeller University Press, New York. 129–141.

Karlish, S. J. D., and W. D. Stein. 1985. Cation activation of the pig kidney sodium pump: transmembrane allosteric effects of sodium. *Journal of Physiology.* 359:119–149.

Karlish, S. J. D., and D. W. Yates. 1978. Tryptophan fluorescence of (Na^+ + K^+)-ATPase as a tool for study of the enzyme mechanism. *Biochimica et Biophysica Acta.* 527:115–130.

Klodos, I., and B. Forbush III. 1988. Rapid conformational changes of the Na/K pump revealed by a fluorescent dye, RH 160. *Journal of General Physiology.* 92:46*a*. (Abstr.)

Klodos, I., and B. Forbush III. 1991. Transient kinetics of dephosphorylation of Na,K-ATPase after dilution of NaCl. *In* The Sodium Pump: Recent Developments. J. H. Kaplan and P. De Weer, editors. The Rockefeller University Press, New York. 327–331.

Klodos, I., and J. G. Nørby. 1988. Does ATP affect the interconversion and the dephosphorylation of the phosphoenzymes of the Na,K-pump? *In* The Na^+,K^+ Pump. Part A: Molecular Aspects. J. C. Skou, J. G. Nørby, A. B. Maunsbach, and M. Esmann, editors. Alan R. Liss, Inc. New York. 321–326.

Läuger, P. 1991. Electrogenic Ion Pumps. Sinauer Associates, Inc. Sunderland, MA. 313 pp.

Läuger, P., and H.-J. Apell. 1986. A microscopic model for the current-voltage behavior of the Na,K-pump. *European Biophysical Journal.* 13:305–321.

Läuger, P., and H.-J. Apell. 1988. Voltage dependence of partial reactions of the Na^+/K^+ pump: predictions from microscopic models. *Biochimica et Biophysica Acta.* 945:1–10.

Läuger, P., W. Lesslauer, E. Marti, and J. Richter. 1967. Electrical properties of bimolecular phospholipid membranes. *Biochimica et Biophysica Acta.* 135:20–32.

Lafaire, A. V., and W. Schwarz. 1986. Voltage dependence of the rheogenic Na^+/K^+ ATPase in the membrane of oocytes of *Xenopus laevis*. *Journal of Membrane Biology.* 91:43–51.

Lowry, O. H., N. J. Rosebrough, A. L. Farr, and R. J. Randall. 1951. Protein measurement with the Folin phenol reagents. *Journal of Biological Chemistry.* 193:265–275.

Mårdh, S., and R. L. Post. 1977. Phosphorylation from adenosine triphosphate of sodium- and potassium-activated adenosine triphosphatase. *Journal of Biological Chemistry.* 252:633–638.

Mårdh, S., and Ö. Zetterquist. 1974. Phosphorylation and dephosphorylation reactions of bovine brain (Na^+ + K^+)-stimulated ATP phosphohydrolase studied by a rapid-mixing technique. *Biochimica et Biophysica Acta.* 350:473–483.

McCray, J. A., L. Herbette, T. Kihara, and D. R. Trentham. 1980. A new approach to time-resolved studies of ATP-requiring biological systems: laser-flash photolysis of caged ATP. *Proceedings of National Academy of Sciences, USA.* 77:7237–7241.

Mezele, M. E., E. Lewitzki, H. Ruf, and E. Grell. 1988. Cation selectivity of membrane proteins. *Berichte der Bunsen-Gesellschaft für Physikalische Chemie.* 92:998–1004.

Nakao, M., and D. C. Gadsby. 1986. Voltage dependence of Na translocation by the Na/K pump. *Nature.* 323:628–630.

Nørby, J. G., and J. Jensen. 1971. Binding of ATP to brain microsomal ATPase. Determination of the ATP-binding capacity and the dissociation constant of the enzyme-ATP complex as a function of K^+-concentration. *Biochimica et Biophysica Acta.* 233:104–116.

Pedemonte, C. H. 1988. Kinetic mechanism of inhibition of the Na^+-pump and some of its partial reactions by external Na^+ (Na_o^+). *Journal of Theoretical Biology.* 134:165–182.

Pratap, P. R., J. D. Robinson, and M. I. Steinberg. 1991. The reaction sequence of the Na^+/K^+-ATPase: rapid kinetic measurements distinguish between alternative schemes. *Biochimica et Biophysica Acta.* 1069:288–298.

Rakowski, R. F., L. A. Vasilets, J. La Tona, and W. Schwarz. 1991. A negative slope in the current-voltage relationship of the Na^+/K^+ pump in *Xenopus* oocytes produced by reduction of external [K^+]. *Journal of Membrane Biology.* 121:171–187.

Rephaeli, A., D. E. Richards, and S. J. D. Karlish. 1986. Conformational transitions in fluorescein-labeled (Na,K)ATPase reconstituted into phospholipid vesicles. *Journal of Biological Chemistry.* 261:6248–6254.

Sachs, J. R. 1981. Mechanistic implications of the potassium-potassium exchange carried out by the sodium-potassium pump. *Journal of Physiology.* 316:263–277.

Schwartz, A., K. Nagano, M. Nakao, G. E. Lindenmayer, and J. C. Allen. 1971. The sodium- and potassium-activated adenosinetriphosphatase system. *Methods of Pharmacology.* 1:361–388.

Shani-Sekler, M., R. Goldshleger, D. M. Tal, and S. J. D. Karlish. 1988. Inactivation of Rb^+ and Na^+ occlusion on (Na^+, K^+)-ATPase by modification of carboxyl groups. *Journal of Biological Chemistry.* 263:19331–19341.

Skou, J. C. 1975. The (Na^+ + K^+)-activated enzyme system and its relationship to transport of sodium and potassium. *Quarterly Reviews on Biophysics.* 7:401–434.

Skou, J. C., and M. Esmann. 1981. Eosin, a fluorescent probe of ATP binding to the (Na^+ + K^+)-ATPase. *Biochimica et Biophysica Acta.* 647:232–240.

Skou, J. C., and M. Esmann. 1983. Effect of magnesium ions on the high-affinity binding of eosin to the (Na^+ + K^+)-ATPase. *Biochimica et Biophysica Acta.* 727:101–107.

Stein, W. D. 1990. Energetics and the design principles of the Na/K-ATPase. *Journal of Theoretical Biology.* 147:145–149.

Steinberg, M., and S. J. D. Karlish. 1989. Studies on conformational changes in Na,K-ATPase labeled with 5-iodoacetamidofluorescein. *Journal of Biological Chemistry.* 264:2726–2734.

Stürmer, W., and H.-J. Apell. 1992. Fluorescence study on cardiac glycoside binding to the Na,K-pump: ouabain binding is associated with movement of electrical charge. *FEBS Letters.* 300:1–4.

Stürmer, W., H.-J. Apell, I. Wuddel, and P. Läuger. 1989. Conformational transitions and charge translocation by the Na,K Pump: comparison of optical and electrical transients by ATP-concentration jumps. *Journal of Membrane Biology.* 110:67–86.

Stürmer, W., R. Bühler, H.-J. Apell, and P. Läuger. 1991*a*. Charge translocation by the Na,K-pump: Ion binding and release studied by time-resolved fluorescence measurements. *In* The Sodium Pump. Recent Developments. J. H. Kaplan and P. De Weer, editors. Rockefeller University Press, New York. 531–536.

Stürmer, W., R. Bühler, H.-J. Apell, and P. Läuger. 1991*b*. Charge translocation by the Na,K-pump: II. Ion binding and release at the extracellular face. *Journal of Membrane Biology.* 121:163–176.

Sweadner, K. J. 1991. Overview: subunit diversity in the Na,K-ATPase. *In* The Sodium Pump: Structure, Mechanism, and Regulation. J. H. Kaplan and P. De Weer, editors. Rockefeller University Press, New York. 63–76.

Taniguchi, K., and R. L. Post. 1975. Synthesis of adenosine triphosphate and exchange between inorganic phosphate and adenosine triphosphate in sodium and potassium ion transport adenosine triphosphatase. *Journal of Biological Chemistry.* 250:3010–3018.

Taniguchi, K., K. Suzuki, and S. Iida. 1983. Stopped flow measurement of conformational change induced by phosphorylation in (Na^+,K^+)-ATPase modified with *N*(*p*-(2-benzimidazolyl)phenyl)maleimide. *Journal of Biological Chemistry.* 258:6927–6931.

Tyson, P. A., M. Steinberg, E. T. Wallick, and T. L. Kirley. 1989. Identification of the 5-iodoacetamidofluorescein reporter site on the Na,K-ATPase. *Journal of Biological Chemistry.* 264:726–734.

Yoda, A., and S. Yoda. 1976. Association and dissociation rate constants of the complexes between various cardiac aglycones and sodium- and potassium-dependent adenosine triphosphatase formed in the presence of magnesium and phosphate. *Molecular Pharmacology.* 13:352–361.

Yoda, A., and S. Yoda. 1987. Two different phosphorylation-dephosphorylation cycles of Na,K-ATPase proteoliposomes accompanying Na^+ transport in the absence of K^+. *Journal of Biological Chemistry.* 262:110–115.